Available online at www.sciencedirect.com
SCIENCE DIRECT®
Fungal Genetics and Biology 41 (2004) 600–623
FUNGAL GENETICS AND BIOLOGY
www.elsevier.com/locate/yfgbi

Genealogical concordance between the mating type locus and seven other nuclear genes supports formal recognition of nine phylogenetically distinct species within the *Fusarium graminearum* clade☆

Kerry O'Donnell,[a,*] Todd J. Ward,[a] David M. Geiser,[b] H. Corby Kistler,[c] and Takayuki Aoki[d]

[a] *Microbial Genomics and Bioprocessing Research Unit, National Center for Agricultural Utilization Research, US Department of Agriculture, Agricultural Research Service, Peoria, IL 61604, USA*
[b] *Department of Plant Pathology, The Pennsylvania State University, University Park, PA 16802, USA*
[c] *Cereal Disease Laboratory, US Department of Agriculture, Agricultural Research Service, 1551 Lindig Street, St. Paul, MN 55108, USA*
[d] *Genetic Diversity Department, National Institute of Agrobiological Sciences (NIAS), 2-1-2 Kannondai, Tsukuba, Ibaraki 305-8602, Japan*

Received 4 December 2003; accepted 5 March 2004

Abstract

Species limits were investigated within the *Fusarium graminearum* clade (*Fg* clade) through phylogenetic analyses of DNA sequences from portions of 11 nuclear genes including the mating-type (MAT) locus. Nine phylogenetically distinct species were resolved within the *Fg* clade, and they all possess contiguous *MAT1-1* and *MAT1-2* idiomorphs consistent with a homothallic reproductive mode. In contrast, only one of the two MAT idiomorphs was found in five other species, four of which were putatively asexual, and the other was heterothallic. Molecular evolutionary analyses indicate the MAT genes are under strong purifying selection and that they are functionally constrained, even in species for which a sexual state is unknown. The phylogeny supports a monophyletic and apomorphic origin of homothallism within this clade. Morphological analyses demonstrate that a combination of conidial characters could be used to differentiate three species and three species pairs. Species rank is formally proposed for the eight unnamed species within the *Fg* clade using fixed nucleotide characters.
Published by Elsevier Inc.

Index Descriptors: Fusarium head blight; Mating-type; Histone H3; Homothallic; Heterothallic; Gene trees; Species trees; Species limits; Phylogeny; Reciprocal monophyly

1. Introduction

Scab or Fusarium head blight (FHB) is an economically devastating disease of wheat and barley that reached epidemic proportions within the United States during the 1990s, resulting in losses of approximately three billion dollars to US agriculture due to poor seed quality and low yields (Windels, 2000). FHB-infected cereal grains may also become contaminated with trichothecene mycotoxins and estrogenic compounds which pose a serious threat to human and animal health and food safety (Miller et al., 1991). FHB is a global problem with recent outbreaks reported in Canada, Europe, Asia, Australia, and South America (McMullen et al., 1997).

The primary causal agent of FHB, *Fusarium graminearum* (teleomorph *Gibberella zeae*), was thought to be a single potentially panmictic species spanning six continents until genealogical concordance phylogenetic species recognition (GCPSR, Taylor et al., 2000) was

☆ Supplementary data associated with this article can be found, in the online version, at doi:10.1016/j.fgb.2004.03.003.

* Corresponding author. Fax: 1-309-681-6672.
E-mail address: kodonnell@ncaur.usda.gov (K. O'Donnell).
URL: http://www.ncaur.usda.gov/MGB/MGB-O'Donnell.htm.

1087-1845/$ - see front matter. Published by Elsevier Inc.
doi:10.1016/j.fgb.2004.03.003

used to investigate species limits using a global collection of FHB strains (O'Donnell et al., 2000; Ward et al., 2002). Results of these studies, based on phylogenetic analyses of DNA sequences from portions of six nuclear genes totaling 7.1 kb, identified eight biogeographically structured, phylogenetically distinct species designated lineages 1–8 (hereafter referred to as the *Fg* clade). All of these lineages appear to have reached an advanced state of genetic isolation because each was reciprocally monophyletic within six individual nuclear gene genealogies and the combined phylogeny of these genes. As predicted by the neutral theory of evolution, in the absence of significant gene flow, genetic drift has eliminated most of the shared neutral polymorphism among the eight lineages at the six loci sampled (O'Donnell et al., 2000). Not surprisingly, significant differences in allelic frequencies have been reported among four of the lineages (Jeon et al., 2003).

To date, GCPSR has been used to investigate species boundaries in a relatively small number of medically (Cruse et al., 2002; Fisher et al., 2002; Kasuga et al., 2003; Koufapanou et al., 1997, 2001; Xu et al., 2000) and agriculturally important fungi (Banke et al., 2004; Carbone et al., 1999; Chaverri et al., 2003; Couch and Kohn, 2002; Craven et al., 2001; Geiser et al., 1998a,b, 2000, 2001; Johannesson and Stenlid, 2003; O'Donnell, 2000; O'Donnell et al., 2000; Rehner and Buckley, 2003; Schardl and Craven, 2003; Steenkamp et al., 2002; Ward et al., 2002), lichens (Kroken and Taylor, 2001; Myllys et al., 2003), and in the model eukaryote *Neurospora* (Dettman et al., 2003a,b). Although sequences of the mating-type (MAT) genes have been hypothesized to "have the potential to mark species boundaries" (Yun et al., 2000), their use for species level phylogenetics has been very limited (Barve et al., 2003; Pöggeler, 1999; Steenkamp et al., 2000; Turgeon, 1998) such that this hypothesis has never been fully tested using GCPSR. Similarily, hypotheses regarding the nature of selective pressure impacting the evolution of MAT have been proposed (Turgeon, 1998), but these genes have never been subjected to rigorous comparative molecular evolutionary analyses.

The present study was conducted to: (1) examine MAT idiomorph evolution within a clade of homothallic, heterothallic, and putatively asexual fusaria; (2) evaluate hypotheses regarding the molecular evolution and phylogenetic utility of MAT genes; (3) extend the previously published (O'Donnell et al., 2000; Ward et al., 2002) analyses of the B trichothecene toxin-producing clade phylogeny (hereafter referred to as the "B clade," which includes the *Fg* clade plus other B-type trichothecene toxin-producing cereal and grass pathogens) using sequences from the MAT locus and histone H3; (4) formally propose species rank for the eight unnamed species within the *Fg* clade, using fixed nucleotide differences (Fisher et al., 2002); and (5) use the combined *Fg* clade phylogeny as a framework for an a posteriori search for species-specific phenotypic characters. For the sake of clarity, and to emphasize the interpretation that the *Fg* clade consists of at least nine species, these newly described species will be referred to by their new epithets throughout this paper.

2. Materials and methods

2.1. Strains

Histories of the strains analyzed phylogenetically and morphologically are listed at http://www.ncaur.usda.gov/MGB/MGB-O'Donnell.htm. This site also contains a list of the primers used for PCR and sequencing, and all of the aligned DNA sequences. All strains are stored in liquid nitrogen vapor at −175 °C and are available upon request from the Agricultural Research Service Culture Collection (NCAUR, Peoria, IL). Strains were cultured and DNA extracted as previously described (O'Donnell et al., 1998a). Because epithets have been given for all 9 species within the *Fg* clade, the following 1–8 lineage designations used formerly have been abandoned (O'Donnell et al., 2000; Ward et al., 2002), but they are listed here as a cross-reference: [1] *Fusarium austroamericanum*, [2] *Fusarium meridionale*, [3] *Fusarium boothii*, [4] *Fusarium mesoamericanum*, [5] *Fusarium acaciae-mearnsii*, [6] *Fusarium asiaticum*, [7] *F. graminearum*, and [8] *Fusarium cortaderiae*. A ninth *Fg* clade species described herein as *Fusarium brasilicum* was not given a lineage designation.

2.2. DNA amplification and sequencing

Primers were designed from GenBank Accession Nos. AF318048 and AF314469–AF314500, to amplify the *MAT1-1* and *MAT1-2* idiomorphs (Yun et al., 2000) and all but 9 codons at either end of the histone H3 gene (Roux et al., 2001), respectively. Platinum *Taq* DNA polymerase Hi-Fi (Invitrogen Life Technologies, Carlsbad, CA) was used to amplify overlapping segments of the MAT locus (Fig. 1) in an Applied Biosystems (ABI, Foster City, CA) 9700 thermocycler, using the following cycling parameters: 94 °C for 90 s, 40 cycles of 94 °C for 30 s, 52 °C for 30 s, 68 °C for 3–5 min, followed by 68 °C for 5 min and a 4 °C soak. Histone H3 was amplified with AmpliTaq (ABI) in a 9700 thermocycler using the following parameters: 94 °C for 30 s, 40 cycles of 94 °C, 52 °C, and 72 °C for 90 s, followed by 10 min at 72 °C and a 4 °C soak. Sequence obtained with the PCR primers was used to design internal sequencing primers (Fig. 1). Amplicons were purified using Montage PCR_{96} Cleanup Filter Plates (Millipore, Billerica, MA) and then cycle-sequenced using ABI BigDye chemistry version 3.0 in a 9700 thermocycler as follows: 96 °C for 15 s,

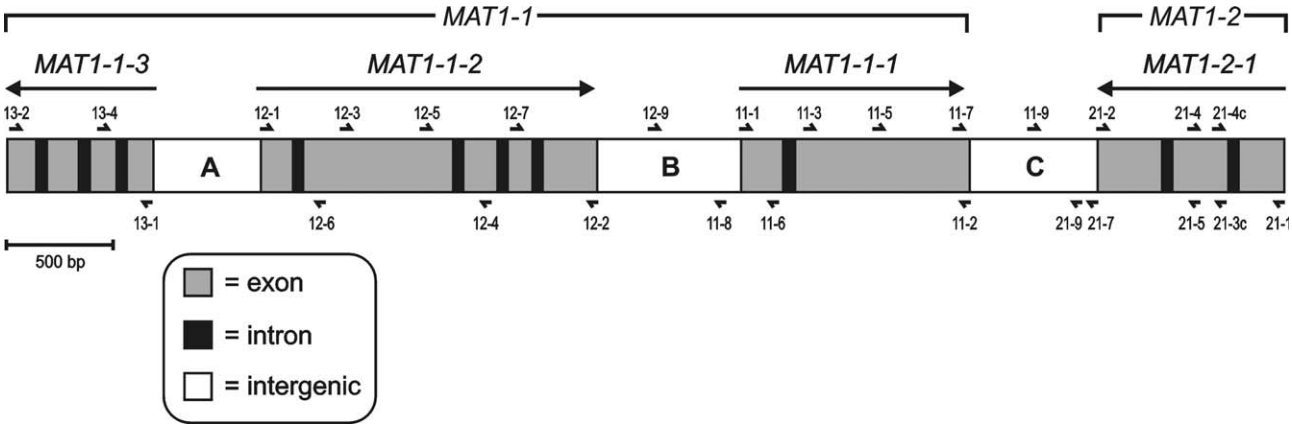

Fig. 1. Map of the mating type (MAT) locus showing exons, introns, and intergenic regions (arbitrarily designated A, B or C). The contiguous arrangement of the *MAT1-1* and *MAT1-2* idiomorphs is typical of homothallic fusaria (Yun et al., 2000). Strains of the single heterothallic species *Fusarium pseudograminearum* and the four putatively asexual species either possess a *MAT1-1* or a *MAT1-2* idiomorph. Idiomorph structure, including intron number and placement, is conserved across the B trichothecene toxin-producing clade. The direction of transcription of each of the four MAT genes is indicated by an arrow. Numbered half-arrows indicate the position of PCR and sequencing primers. Primer sequences are available at http://www.ncaur.usda.gov/MGB/MGB-O'Donnell.htm.

40 cycles of 96 °C for 15 s, 50 °C for 10 s, 60 °C for 4 min, and ending in a 4 °C soak. Sequencing reactions were purified via ethanol precipitation and then run on an ABI 377, 3100 or 3730 genetic analyzer. DNA sequences were edited using Sequencher ver. 4.1.2 (Gene Codes, Ann Arbor, MI) and alignments were improved manually. Sequences have been deposited in the GenBank database under Accession Nos. AF212435–AF212825 (O'Donnell et al., 2000), AY222642 and AY225882–AY225898 (Ward et al., 2002), and AY452807–AY452980 for sequences generated in the present study.

2.3. Determination of mating type

A multiplex PCR was used to screen strains of the following heterothallic and putatively asexual B clade species, using primers M12-1 × M12-2 for the *MAT1-1* idiomorph and M21-1 × M21-2 for the *MAT1-2* idiomorph (Fig. 1): *Fusarium culmorum* (39 strains), *Fusarium cerealis* (50 strains), *Fusarium lunulosporum* (1 strain), *F. pseudograminearum* (53 strains), and the undescribed *Fusarium* sp. NRRL 29298 and 29380 *ex Dactylis glomerata* (orchard grass, 2 strains). The PCR cycling profile used for the MAT idiomorph test was identical to the one listed above for Platinum *Taq* DNA polymerase Hi-Fi except that the extension time was reduced to 2 min at 68 °C. A complete listing of the strain histories and MAT idiomorph determinations can be found at http://www.ncaur.usda.gov/MGB/MGB-O'Donnell.htm.

2.4. Phylogenetic analysis

All phylogenetic analyses were conducted with PAUP* ver. 4.0b10 (Swofford, 2002; Table 1). Phylogenetically informative indels were coded as single events. Two hundred and twenty-nine ambiguously aligned nucleotide positions within the intergenic B region of the MAT locus were excluded from the analyses. Based on the results of more inclusive phylogenetic analyses that included members of the A trichothecene toxin-producing clade, sequences of *Fusarium pseudograminearum* and *Fusarium* sp. 29380 were used to root the individual and combined datasets, except for the analysis of the MAT locus, which was midpoint rooted because these two species were not resolved as sister taxa within this partition. Although there is no obvious explanation for this topology, it does not impact the main points of this paper.

Searches for the most-parsimonious trees used a heuristic search with 1000 random addition replicates and tree bisection with reconnection branch swapping, after excluding ambiguously aligned nucleotide positions. The Templeton WS-R test implemented in PAUP* was used to assess whether the various gene partitions could be combined, after excluding the three strains that only possess a *MAT1-2* idiomorph (i.e., *F. cerealis* NRRL 13721 and 25491 and *F. culmorum* NRRL 3288). We used 70% bootstrap majority rule trees from each of the following datasets as constraints: histone, MAT and non-MAT without histone. Results for all of the Kishino–Hasegawa (K–H) tests ($P = 1.0$) indicated these datasets could be combined. Clade stability was assessed via parsimony bootstrapping in PAUP*, using a heuristic search with 1000 pseudoreplications of the data and 10 random addition sequences per replicate, and tree bisection with reconnection branch swapping. Decay indices were calculated with AutoDecay ver. 4.0 (Eriksson, 1998). Monophyly of the nine *Fg* clade species, *F. culmorum*, *F. cerealis*, and *F. pseudograminearum* was also assessed by enforcing topological constraints on the combined dataset that

Table 1
Tree statistics and summary sequence for the individual and combined partitions[a]

Locus	# bp/aa[b]	PIC	PIC/bp or aa	Autapo	% Variable	# MPTs	Length	CI	RI
MAT1-1-3 gene[c]	662	55	8.3	15	10.6	4	79	0.9241	0.9766
Intergenic A[c]	514	88	17.1	34	23.7	26	143	0.9301	0.9791
MAT1-1-2 gene[c]	1582	114	7.2	46	10.1	2	177	0.9379	0.9818
Intergenic B[c,d]	629	93	14.8	34	20.2	16	151	0.9007	0.9711
MAT1-1-1 gene[c]	1091	58	5.3	27	7.8	10	106	0.8396	0.9549
Intergenic C[e]	611	35	5.7	3	6.2	3840	62	0.6774	0.9115
MAT1-2-1 gene[f]	841	39	4.6	7	5.5	747	57	0.8246	0.9225
MAT locus combined[g]	5930[d]	464 (482)	7.8 (8.1)	112 (166)	9.7 (10.9)	120 (147,900)	781 (804)	0.8489 (0.8532)	0.9539 (0.9544)
MAT1-1 idiomorph	5319[c]	429	8.1	159	11.0	5	704	0.8821	0.9644
MAT protein[c]	1228 aa	73	5.9/aa	22	7.7	6	123	0.9024	0.9740
Histone H3	449	36	8.0	11	10.5	4	56	0.8750	0.9581
All loci (except MAT)[h]	7708	636	8.35	256	11.6	18	1169	0.7956	0.9217
All loci combined	13,638[d]	1117	8.2	422	11.3	2	2044	0.7906	0.9241

[a] *Abbreviations used:* PIC, parsimony informative character or synapomorphy (i.e, a shared derived character); Autapo, autapomorphy or a derived character state unique to a particular taxon; MPTs, most-parsimonious trees; CI, consistency index; RI, retention index.

[b] Note that all values given are for nucleotides except for the MAT protein.

[c] *MAT1-2* only strains excluded (i.e., *F. cerealis* NRRL 13721 and 25491 and *F. culmorum* NRRL 3288).

[d] 229 ambiguously aligned nucleotide positions within intergenic-B excluded.

[e] *MAT1-1* and *MAT1-2* only strains excluded.

[f] *MAT1-1* only strains excluded.

[g] Analyzed with *MAT1-2* only strains excluded or included (in parentheses).

[h] Includes previously published data from the following six housekeeping genes (O'Donnell et al., 2000; Ward et al., 2002) (listed by locus, bp sequenced, PIC/bp, and % bp variable): translation elongation factor (1α) 648 bp, 8.5 and 10.6%; reductase, 1154 bp, 10.6 and 18.4%; phosphate permase, 886 bp, 11.3 and 15%; *Tri101*, 1336 bp, 7.9 and 10.4%; ammonia ligase, 1902 bp, 8.4 and 11.5%; and β-tubulin, 1333 bp, 4.2 and 5.5%.

were incompatible with the monophyly of each of these species. The significance of differences between optimal (most-parsimonious) and constraint trees was evaluated using the K–H tests implemented in PAUP*. DnaSP ver. 3.99 (Rozas et al., 2003) and MEGA ver. 2.1 (Kumar et al., 2001) were used, respectively, to estimate DNA polymorphism within and among species and to estimate DNA divergence between species.

2.5. Analysis of MAT molecular evolution

Patterns of selective pressure within MAT genes were investigated by using codon models of molecular evolution (Goldman and Yang, 1994; Yang, 1998; Yang et al., 2000) to derive maximum likelihood estimates of the nonsynonymous/synonymous (d_N/d_S) rate ratio, ω. A gene evolving in a neutral fashion will fix amino acid changes at the same rate as synonymous substitutions, and ω will be approximately 1. Purifying selection is inferred when ω is significantly less than 1, and positive selection is indicated when ω is significantly greater than 1. Maximum likelihood analyses were performed with PAML ver. 3.13 (Yang, 1997), using single representatives of each species, and fully bifurcating phylogenetic trees inferred as described above. In addition to the sequences used in the broader phylogenetic analyses, the nucleotide sequence of the *MAT1-2-1* gene from *F. pseudograminearum* (NRRL 28069) was added to the datasets used for maximum likelihood analyses of selective pressure. The relative fit of codon models to individual data partitions was examined using likelihood ratio tests, which compared twice the log-likelihood difference between models with a χ^2 distribution having degrees of freedom equal to the difference in the numbers of free parameters between models. Average ω values for intraspecific comparisons were estimated using the modified Nei–Gojobori model (Zhang et al., 1998) with Jukes–Cantor distances. Intraspecific analyses were performed with MEGA ver. 2.1 (Kumar et al., 2001), using a combined MAT dataset consisting of species represented by at least two sequences from each of the MAT genes.

2.6. Phenotypic analysis

Strains were compared phenotypically as described in Aoki and O'Donnell (1999a). Strains were grown at 25 °C on potato dextrose agar (Difco, Detroit, MI) in 9 cm plastic Petri dishes in the dark in order to assess colony morphology, color, and odor. Microscopic examination and measurements were made on cultures grown on synthetic low nutrient agar (SNA; Aoki and O'Donnell, 1999a). Cultures were incubated on SNA up to 7 days at 25 °C under continuous black light to induce constant conidiogenesis. The length, width, and widest position of 50 5-septate conidia randomly selected from

each culture were measured. A dried culture of each new species described in the present study has been deposited as the holotype in the US National Fungus Collection (BPI), USDA/ARS, Beltsville, MD, USA.

3. Results

3.1. Structural organization of the B clade MAT locus

PCR primers were designed from GenBank Accession No. AF318048 *F. graminearum* GZ3639 = NRRL 29169 (Fig. 1) to amplify the entire coding region of the *MAT1-1* and/or *MAT1-2* idiomorphs from 47 strains chosen to represent the known genetic diversity of the B trichothecene toxin-producing clade of *Fusarium*. DNA sequence analysis revealed that structural organization of the MAT locus in the 36 strains representing the nine phylogenetic species of the *Fg* clade is identical to that reported for the homothallic strain GZ3639 (Yun et al., 2000). By way of contrast, strains of the four putatively asexual species (*F. lunulosporum*, *F. cerealis*, *F. culmorum*, and *Fusarium* sp. NRRL 29380), and the heterothallic *F. pseudograminearum* (teleomorph = *Gibberella coronicola*; Aoki and O'Donnell, 1999b) possess either a *MAT1-1* or *MAT1-2* idiomorph. The four strains of *F. pseudograminearum* and the single strain of *F. lunulosporum* and *Fusarium* sp. NRRL 29380 included in the phylogenetic analyses only possess a *MAT1-1* idiomorph, whereas strains of *F. culmorum* and *F. cerealis* possess either a *MAT1-1* or *MAT1-2* idiomorph, but not both. Primer pairs M12-1 × M12-2 and M21-1 × M21-2 (Fig. 1) were used in a multiplexed PCR as a screen for the *MAT1-1* and *MAT1-2* idiomorphs, respectively. With this screen, each pair of interfertile strains of *F. pseudograminearum* used in crosses to obtain the teleomorph (Aoki and O'Donnell, 1999b) included a *MAT1-1* and a *MAT1-2* strain. When this idiomorph test was used to screen a global collection of one heterothallic (i.e., *F. pseudograminearum*) and two putatively asexual species (i.e., *F. cerealis* and *F. culmorum*), all three showed a nearly equal frequency of both idiomorphs (*F. pseudograminearum* 25:28, *F. cerealis* 25:25, and *F. culmorum* 21:18).

Comparison of the MAT locus sequence from *F. graminearum* NRRL 29169 to the sequence of the same strain in GenBank (AF318048; Yun et al., 2000) identified five differences in the published sequence at the following nucleotide positions (Fig. 1): 4254 in the *MAT1-1-3* gene, 6405 in intergenic B, 8394 and 8590 in intergenic C, and 8762 in the *MAT1-2-1* gene. Our sequence specifies a different codon (CAA instead of CAG), but the same amino acid (glutamine), in *MAT1-2-1* and a different amino acid (tyrosine instead of histidine) in *MAT1-1-3*. We believe that our sequence is correct because this tyrosine residue is fixed throughout the B clade.

We were able to assess polymorphisms throughout the MAT region, except the sequence to which the PCR primers annealed. The annealing sites covered 8 codons at the 3′ end of the *MAT1-1-3* gene and another 8 codons at the 5′ end of the *MAT1-2-1* gene (Fig. 1). Novel features of the hypothetical translated MAT proteins, including stop codons at amino acid positions 405 (TAA), 422 (TAA), and 448 (TAG) near the 3′ end of the *MAT1-1-2* protein of *F. cerealis*, *F. culmorum*, and *F. pseudograminearum* and a stop codon at position 405 in the *MAT1-1-2* protein of *F. lunulosporum* and *Fusarium* sp. 29380 (Fig. 2), suggest this truncated protein may represent the pleisomorphic condition within the B clade. By way of contrast, the translated *MAT1-1-2* protein shared by the *Fg* clade species is predicted to contain 59 additional amino acids at the carboxyl terminus, except for strains of *F. boothii*, which have a frame shift mutation at position 405 due to a single base pair deletion. As a result, strains of this species are predicted to possess 47 divergent amino acids at the carboxy-terminus. Another noteworthy feature is that the translated *MAT1-1-1* protein of *F. pseudograminearum*, *F. cerealis*, *F. culmorum*, and *F. lunulosporum* contains 343 amino acids rather than 345 due to the deletion of codons 167 and 168 which encode theronine and methionine in all other members of the B clade.

3.2. Molecular evolution of MAT

Likelihood scores and estimates of ω under different models of codon evolution are listed in Table 2. Using

```
                                        405                                                                 463
                                         |                                                                   |
Fg clade [except F. boothii]  YSPVVSKQLFKSSFVLFPDSNLVCIRSKSPVQMRLEILVSLSCPQPFTLWGLTMTLRSRMMVSSL*
F. boothii                    YSPVVSNSCSKVPLFHSLILIWYALDPKAPRRCGWKSWSPFHVHSRSRFGGSR*P*GAG*WFLHY
F. lunulosporum               YSPVVS*QLFKSLFVSFSDSSFVYIRSKSPVQMRLEILVSLSCPPPFTLWELTMTLRSRMMVSSL*
F. culmorum                   YSPVVS*QLFKSPFVSFSDSNFV*IRSKSPVQMRLEILVSLSCPPPFTL*ELTMTLRSRMMVSSL*
F. cerealis                   YSPVVS*QLFKSPFVSFSDSNFV*IRSKSPVQMRLEILVSLSCPPPFTL*ELTMTLRSRMMVSSL*
F. pseudograminearum          YSPVVS*QLFKSPFVSFSDSNFV*IRSKSPVQMRLEILVSLSCPPPFTL*ELTMTLRSRMMVSSL*
Fusarium sp. 29380            YSPVVS*QLFKTPFVSFSDSNFVCIRSKSPVQMRLEILVSLSCPPLFTLWELTMTLRSRMMVSSL*
```

Fig. 2. Amino acid alignments of the carboxy-terminus of the *MAT1-1-2* protein showing stop codons (indicated by bold asterisks) in the sequence of *Fusarium cerealis*, *F. culmorum*, *F. pseudograminearum*, *F. lunulosporum*, and *Fusarium* sp. 29380. The *MAT1-1-2* protein in all of the *Fg* clade species is predicted to contain 463 amino acids, except for strains of *F. boothii* which have a frame shift mutation at position 405 due to a single base pair deletion. As a result, strains of this species are predicted to possess 47 divergent amino acids at the carboxy-terminus.

Table 2
Parameter estimates and likelihood scores for MAT genes

Gene	Model	p	Estimates of ω	$-\ln L$
MAT1-1-1	One-ratio (M0)	1	$\omega = 0.18$	1949.75
	Neutral (ω fixed at 1)	0	$\omega = 1.00$ (fixed)	1979.90
	Discrete (M3)	3	$\omega_0 = 0.00$, $f_0 = 0.87$ $\omega_1 = 1.41$, $f_1 = 0.13$	1939.00
	Beta (M7)	2	$p = 0.00$, $q = 0.01$	1939.76
	Beta&ω (M8)	4	$p = 0.00$, $q = 0.02$, $f_0 = 0.95$ $\omega_1 = 1.74$, $f_1 = 0.05$	1939.08
	HH3	3	$\omega_{HET} = 0.16$, $\omega_{HOMO} = 0.23$ $\omega_{EQUIV}0.15$	1949.42
MAT1-1-2	One-ratio (M0)	1	$\omega = 0.22$	2286.77
	Neutral (ω fixed at 1)	0	$\omega = 1.00$ (fixed)	2314.09
	Discrete (M3)	3	$\omega_0 = 0.08$, $f_0 = 0.90$ $\omega_1 = 1.50$, $f_1 = 0.10$	2282.07
	Beta (M7)	2	$p = 0.02$, $q = 0.05$	2282.15
	Beta&ω (M8)	4	$p = 9.15$, $q = 99.00$, $f_0 = 0.90$ $\omega_1 = 1.51$, $f_1 = 0.10$	2282.07
	HH3	3	$\omega_{HET} = 0.19$, $\omega_{HOMO} = 0.32$ $\omega_{EQUIV} = 0.18$	2286.14
MAT1-1-3	One-ratio (M0)	1	$\omega = 0.32$	1078.27
	Neutral (ω fixed at 1)	0	$\omega = 1.00$ (fixed)	1086.72
	Discrete (M3)	3	$\omega_0 = 0.00$, $f_0 = 0.75$ $\omega_1 = 1.30$, $f_1 = 0.25$	1074.54
	Beta (M7)	2	$p = 0.00$, $q = 0.01$	1074.68
	Beta&ω (M8)	4	$p = 0.00$, $q = 1.79$, $f_0 = 0.75$ $\omega_1 = 1.29$, $f_1 = 0.25$	1074.54
	HH3	3	$\omega_{HET} = 0.25$, $\omega_{HOMO} = 0.42$ $\omega_{EQUIV} = 0.41$	1077.87
MAT1-2-1	One-ratio (M0)	1	$\omega = 0.27$	1334.19
	Neutral (ω fixed at 1)	0	$\omega = 1.00$ (fixed)	1343.87
	Discrete (M3)	3	$\omega_0 = 0.08$, $f_0 = 0.92$ $\omega_1 = 2.76$, $f_1 = 0.08$	1328.05
	Beta (M7)	2	$p = 0.00$, $q = 0.01$	1328.98
	Beta&ω (M8)	4	$p = 8.28$, $q = 99.0$, $f_0 = 0.92$ $\omega_1 = 2.77$, $f_1 = 0.08$	1328.05
	HH3	3	$\omega_{HET} = 0.39$, $\omega_{HOMO} = 0.21$ $\omega_{EQUIV} = 0.07$	1332.76

p, the number of free parameters; ω_{HET}, parameter estimate for heterothallic/putatively asexual branches of the phylogeny; ω_{HOMO}, parameter estimate for homothallic branches of the phylogeny; ω_{EQUIV}, parameter estimate for the equivocal branch of the phylogeny; $-\ln L$, likelihood score.

model M0, which assumes a single ω ratio for all nucleotide sites and all branches of a phylogeny, ω estimates were $\geqslant 0.32$ for each of the MAT genes. LRTs demonstrated that M0 provided a significantly better fit to the data from each of the MAT genes ($P < 0.001$) than did a model in which ω was fixed at 1 (neutral expectation), indicating that the molecular evolution of all four MAT genes differs significantly from neutral expectations and is dominated by purifying selection (Table 3). Estimates of selective pressure based on intraspecific comparisons of the combined MAT data (average $\omega = 0.31$) were consistent with the results of interspecific comparisons, indicating that MAT genes were subject to strong purifying selection within the B clade.

Significant variation in selective constraints among sites ($P < 0.05$) was identified in each of the MAT genes by comparing the site homogeneous model (M0) with a discrete model (M3), which allowed two site classes with independent ω ratios (Table 3). A discrete model with three site classes was also tested (data not shown), but failed to provide a better fit to the data than the model with two site classes. While parameter estimates under model M3 further indicated that all MAT genes were dominated by strong purifying selection, with the majority of sites having $\omega \leqslant 0.08$, a subset of sites within each of the four genes had $\omega > 1.0$ (Table 2). However, LRTs specific for positive selection at individual sites, performed by comparing site-heterogeneous models that either prohibit (M7) or allow (M8) positively selected sites, were not significant ($P \geqslant 0.39$) for any of the MAT genes (Table 3). The failure of the M8 model to provide a significant improvement over M7 indicates that there is no statistical support for positive selection at individual sites within the MAT genes, and is consistent with the interpretation that ω_1 from model M3 (Table 2)

Table 3
Likelihood ratio test results

Gene	LRT	2δ	df	*P*-value
MAT1-1-1	M0 vs. Neutral	60.30	1	8.14E-15
	M0 vs. M3	21.5	2	2.14E-5
	M7 vs. M8	1.36	2	0.51
	M0 vs. HH3	0.66	2	0.72
MAT1-1-2	M0 vs. Neutral	54.64	1	1.45E-13
	M0 vs. M3	9.4	2	0.01
	M7 vs. M8	0.16	2	0.92
	M0 vs. HH3	1.26	2	0.53
MAT1-1-3	M0 vs. Neutral	16.90	1	3.94E-5
	M0 vs. M3	7.48	2	0.02
	M7 vs. M8	0.28	2	0.87
	M0 vs. HH3	0.8	2	0.67
MAT1-2-1	M0 vs. Neutral	19.36	1	1.08E-5
	M0 vs. M3	12.28	2	2.15E-3
	M7 vs. M8	1.86	2	0.39
	M0 vs. HH3	2.86	2	0.24

δ, log-likelihood difference between models.

indicates a fraction of neutrally evolving sites within these genes.

To examine possible differences in selective constraint between the homothallic and heterothallic/putatively asexual fusaria examined, LRTs were performed that compared M0 with a branch-specific model, HH3, that allowed for estimation of separate ω ratios for homothallic branches, heterothallic/putatively asexual branches, and a branch leading to the *Fg* clade that is equivocal with respect to reproductive lifestyle and MAT organization (Fig. 6). Although estimates of ω were lower (indicating greater selective constraint) among heterothallic/putatively asexual branches than homothallic branches for the three genes in the *MAT1-1* idiomorph, the opposite was true for the *MAT1-2* idiomorph, and LRTs of the M0 versus HH3 models were not significant ($P > 0.23$) for any of the MAT genes (Table 3). Branch models were also used to determine that $\omega < 1$ along terminal branches leading to each of the heterothallic/putatively asexual species individually. Taken together, these results demonstrate that selective pressure on MAT is essentially equivalent between the homothallic and heterothallic/putatively asexual fusaria examined, and indicate that the molecular evolution of MAT is functionally constrained, even in B clade species where a sexual state has not been identified.

3.3. MAT and multilocus phylogeny of the B clade

Tree statistics and summary sequence for the individual and combined partitions are listed in Table 1. Overall, the combined MAT sequence, which includes 5930 aligned nucleotide positions after excluding 229 ambiguously aligned positions within intergenic B, and those from all other loci combined (7708 aligned nucleotide positions) possess nearly identical phylogenetic signal as measured by parsimony informative characters (PIC) per bp. Within the MAT locus, intergenic A and B possess 2–3 times more PIC/bp as compared with the four genic regions. Intergenic C, which bridges the *MAT1-1* and *MAT1-2* idiomorphs, is the least informative intergenic region and the most homoplasious (CI = 0.6674). Comparisons among the four MAT genes show that *MAT1-1-3* and *MAT1-1-2* are the most informative and least homoplasious. The non-MAT sequence data consists of portions of six previously published nuclear genes (O'Donnell et al., 2000; Ward et al., 2002). Sequences from these genes were collected for the newly discovered *Fg* clade species *F. brasilicum* in Brazil *ex* oats and barley and *Fusarium* sp. NRRL 29380 *ex* orchard grass (*Dactylis glomerata*) in Oregon. A histone H3 dataset consisting of 449 aligned nucleotide characters was added to the non-MAT dataset. Physical locations of the genes with their automatically assigned protein number designations (in parentheses), derived from the genome sequence of *F. graminearum* (PH1 = NRRL 31084) and the genetic map of Gale et al. (http://www.broad.mit.edu/annotation/fungi/fusarium/maps.html), are as follows: scaffold 2—histone H3 (FG04290.1) and reductase (FG03224.1); scaffold 4—phosphate permase (FG07894.1), *Tri101* (FG07896.1) and ammonia ligase; scaffold 5—*MAT1-1-3* (FG08890.1), *MAT1-1-2* (FG08891.1), *MAT1-1-1* (FG08892.1), *MAT1-2-1* (FG08893.1), and translation elongation factor 1α (FG08811.1); scaffold 6—β-tubulin (FG09530.1).

Of the eleven genic regions sequenced, histone is the smallest but it possesses as much phylogenetic signal measured as PIC/bp as the most informative gene sequenced (Table 1). Parsimony analysis of the histone H3 dataset produced four most-parsimonious trees of 56 steps (Fig. 3), in which a monophyletic origin of the *Fg* clade was strongly supported (100% bootstrap). However, due to its small size with only 36 PIC, only four of the nine *Fg* clade species were recovered in >70% of the bootstrap replicates. Maximum parsimony analysis of the aligned DNA sequences from the MAT locus (5930 bp; Fig. 4), the non-MAT loci (7708 bp; Fig. 5), and all loci combined (13,638 bp; Fig. 6) resolved the same nine strongly supported (98–100% bootstrap value), biogeographically structured, reciprocally monophyletic species within the *Fg* clade. The only potential conflict between the MAT and non-MAT partitions within the *Fg* clade involved the phylogenetic relationship of *F. acaciae-mearnsii*. This species received modest bootstrap support as a sister to a South American subclade comprising (*Fusarium meridioniale* (*F. austro-americanum* (*F. cortaderiae*, *F. brasilicum*))) (80% bootstrap) and *F. asiaticum* and *F. graminearum* (75% bootstrap) in the MAT and non-MAT gene trees, respectively. Although the *Fg* clade *F. meridionale* × *F. asiaticum* hybrid strain NRRL 28721 was resolved as

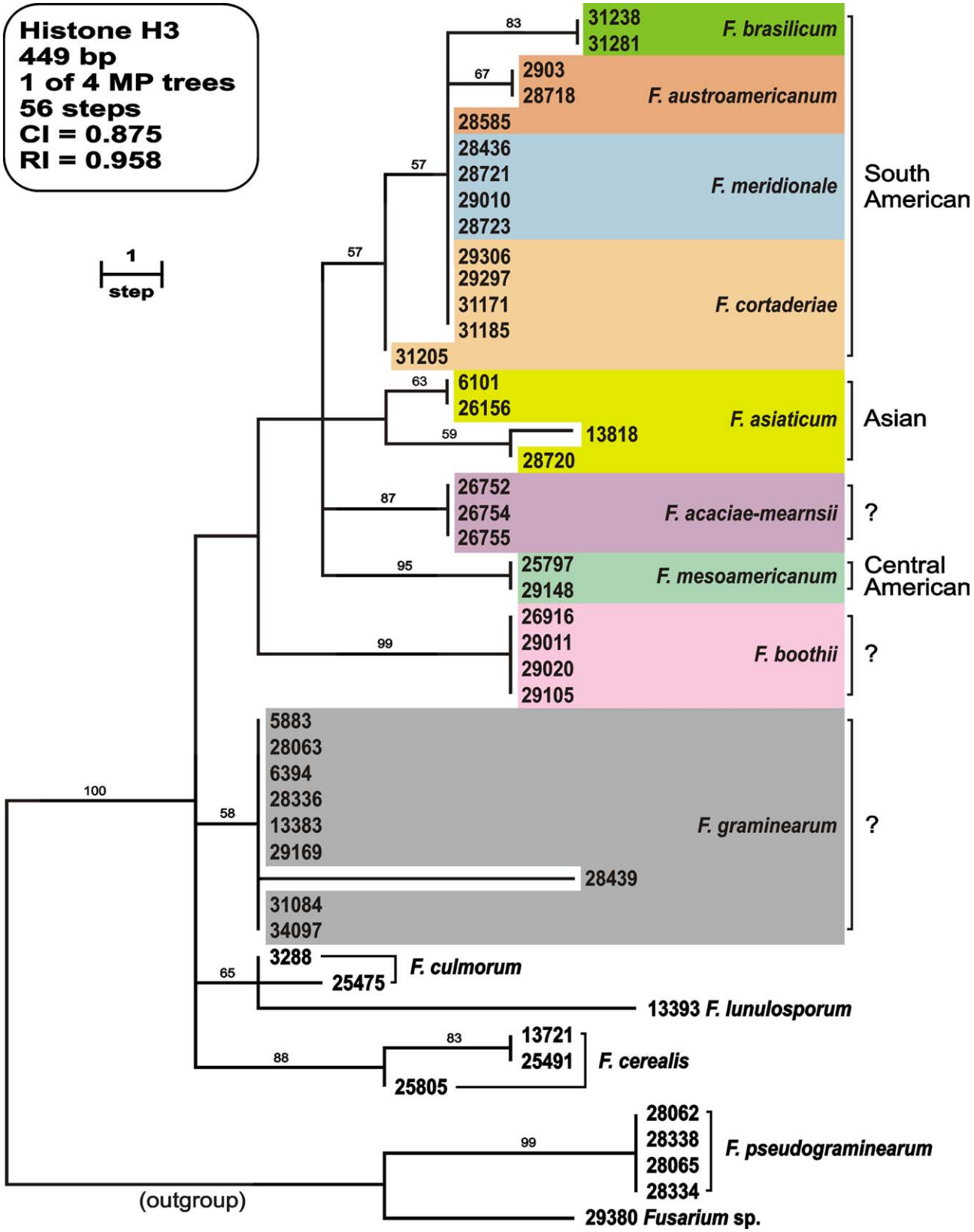

Fig. 3. One of four single most-parsimonious phylograms inferred from the histone H3 sequence data rooted with sequences of *Fusarium pseudograminearum* and *Fusarium* sp. 29380. The nine species of the *Fg* clade are color-coded and the putative endemic area for six of the nine species is indicated. Bootstrap values >50% are indicated above internodes.

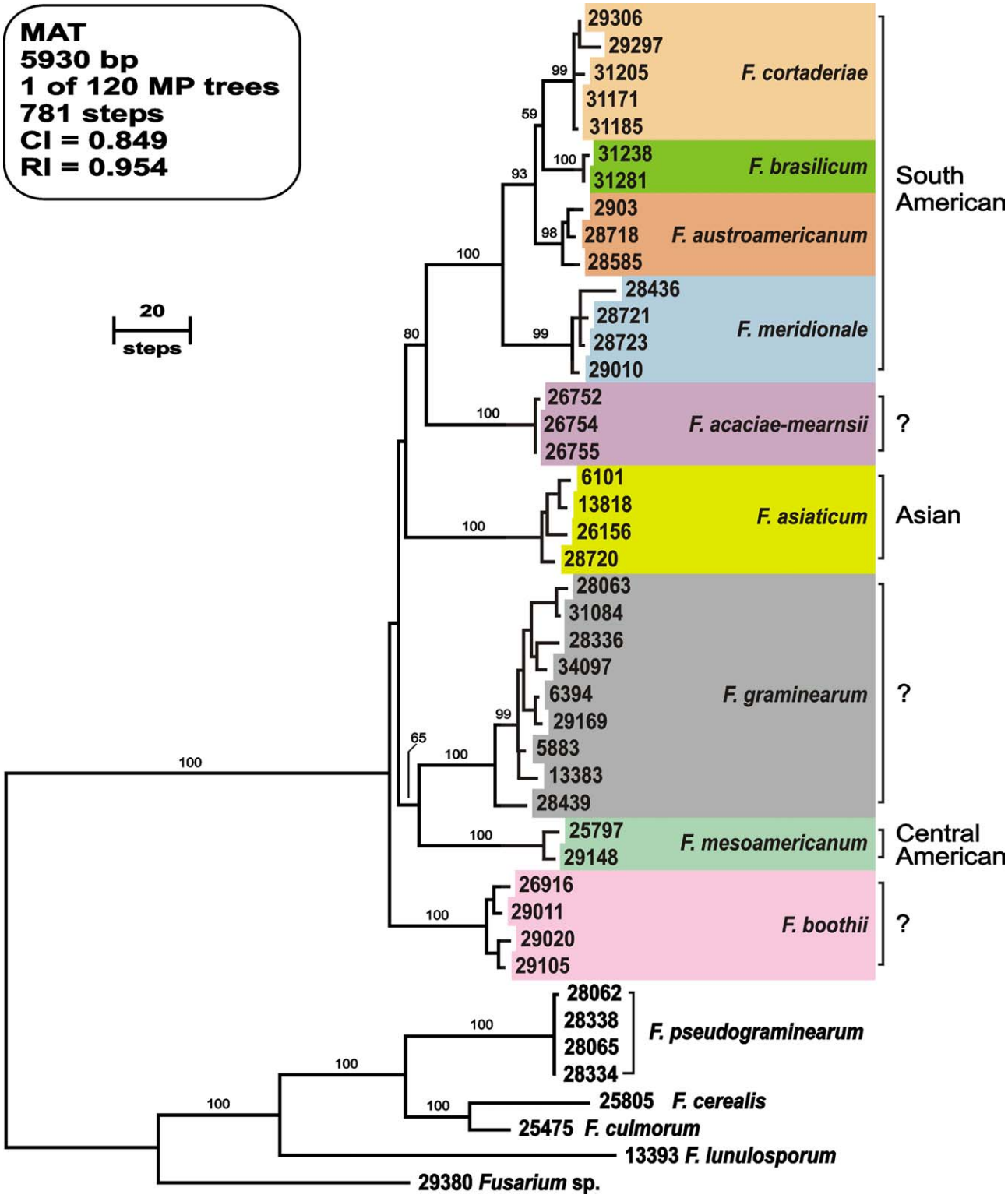

Fig. 4. One of 120 most-parsimonious phylograms inferred from the MAT sequence data. The tree was midpoint rooted because *Fusarium pseudograminearum* and *Fusarium* sp. 29380 were not resolved as sister taxa within the MAT phylogeny. *Fg* clade species are color-coded and the putative endemic area of six of the species is indicated. Bootstrap values >50% from 1000 replications are indicated above internodes.

the basal most member of the most derived parent *F. asiaticum* in the non-MAT phylogeny (Fig. 5), as previously reported (O'Donnell et al., 2000), this strain possesses *F. meridionale* MAT idiomorphs (Fig. 4), and it was resolved cladistically as the earliest diverging branch within *F. meridionale* in the combined phylogeny (Fig. 6).

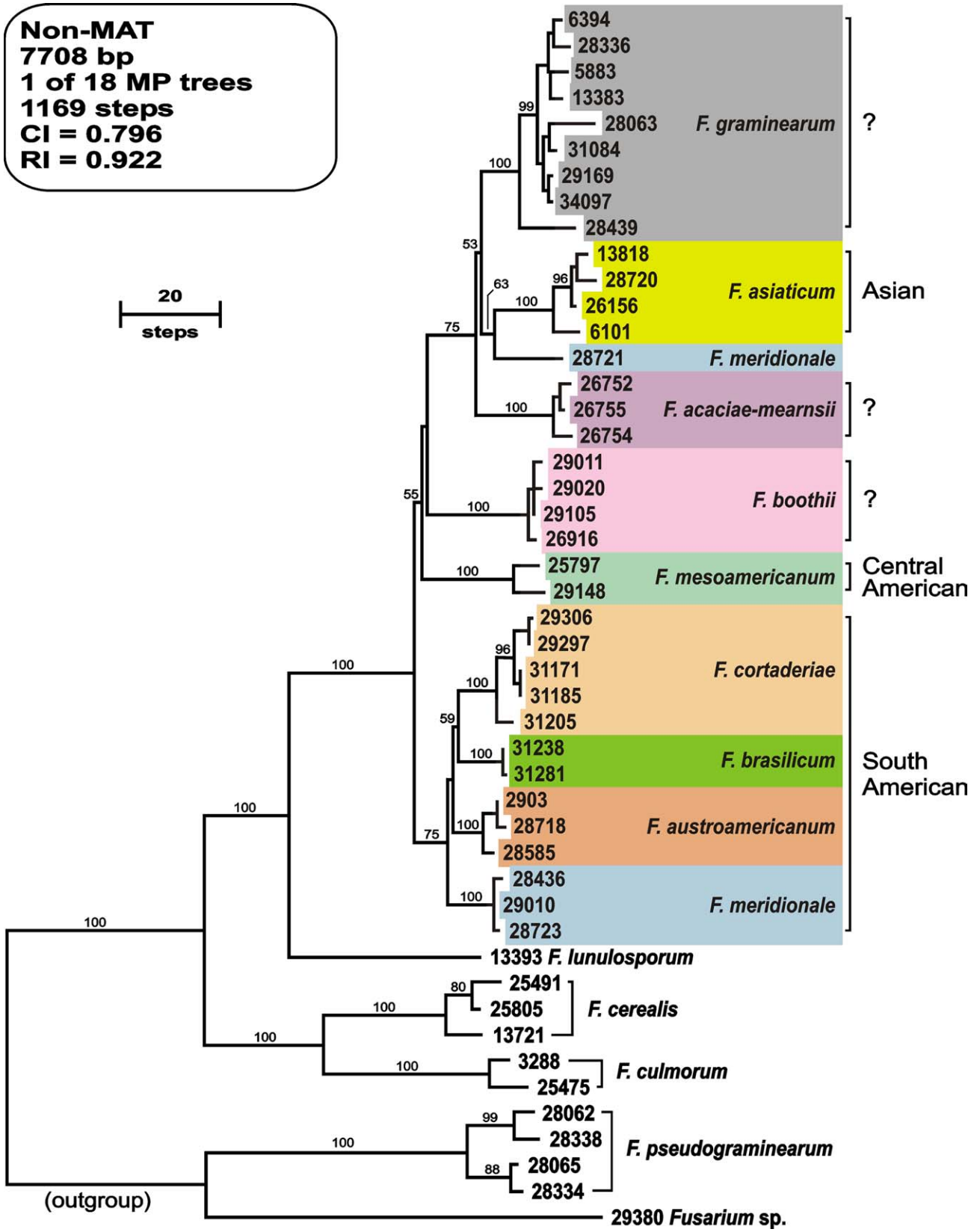

Fig. 5. One of 18 most-parsimonious phylograms inferred from the combined non-MAT data consisting of portions of seven nuclear genes rooted using sequences of *Fusarium pseudograminearum* and *Fusarium* sp. 29380. The putative area of endemism for six of the nine color-coded species in the *Fg* clade is indicated. The hybrid strain *F. meridionale* NRRL 28721 was resolved cladistically as the basal most member of the most derived parent, *F. asiaticum*. Numbers above internodes indicate bootstrap values >50%.

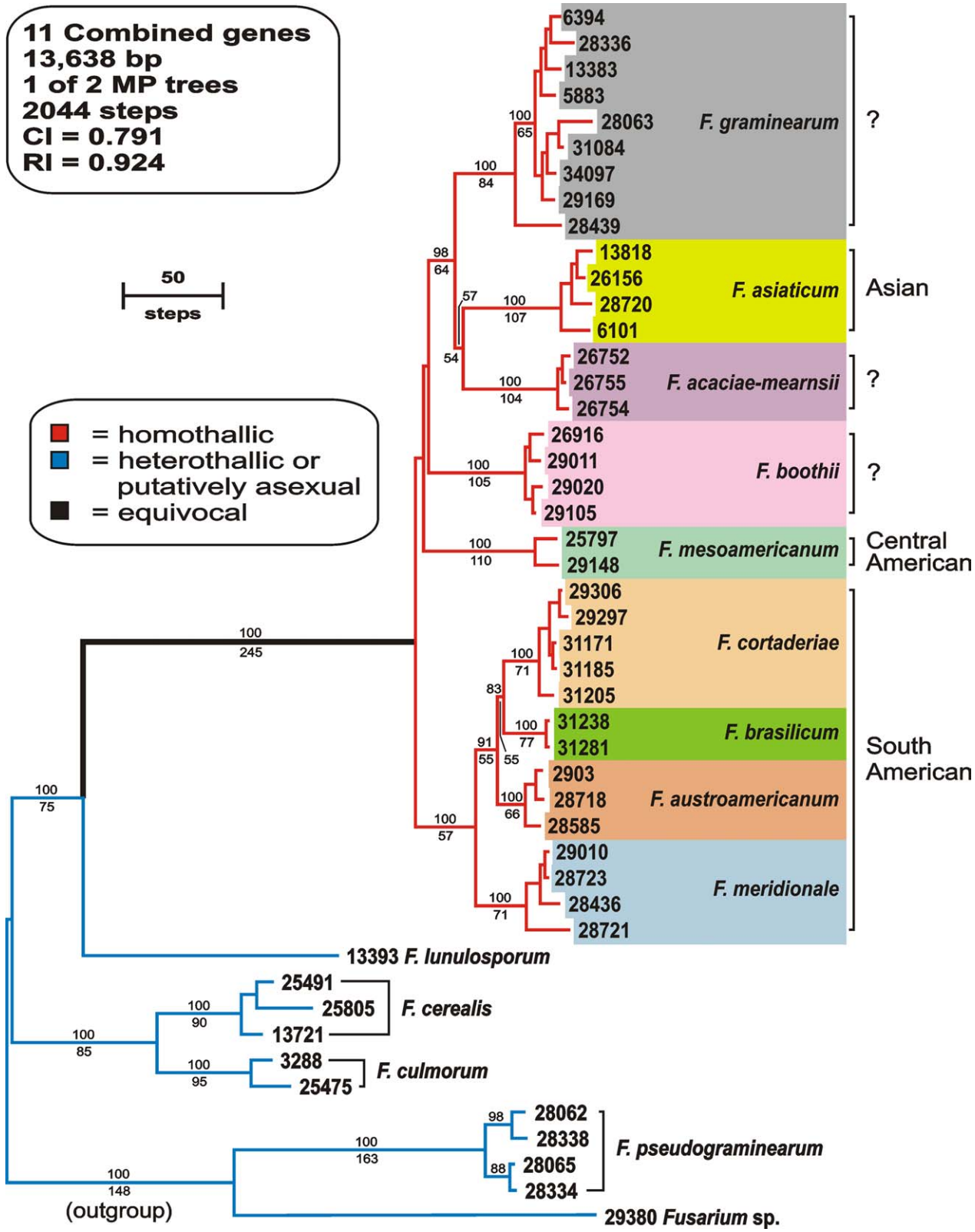

Fig. 6. One of two most-parsimonious phylograms inferred from the combined MAT and non-MAT data consisting of portions of eleven nuclear genes rooted with sequences of *Fusarium pseudograminearum* and *Fusarium* sp. 29380. The putative endemic area for six of the nine color-coded *Fg* clade species is indicated. Branches are color-coded to indicate whether reproductive mode is equivocal, homothallic or heterothallic or putatively asexual. *F. pseudograminearum* in the only known heterothallic species within the B trichothecene toxin-producing clade (Aoki and O'Donnell, 1999b). Note that the branch leading to homothallism is coded as equivocal to indicate uncertainty as to when this reproductive mode arose along this internode. Bootstrap values >50% are indicated above internodes; decay indices are indicated below internodes.

The individual and combined partitions all strongly support a monophyletic origin of the *Fg* clade and homothallism (100% bootstrap; decay index = 245). The combined phylogeny (Fig. 6) is considered to represent the best estimate of B clade evolution because more internodes were supported and they received higher bootstrap scores, the K–H test results of the non-monophyly constraints were significantly worse than the most-parsimonious trees (MPTs) at $P < 0.0001$, the two most-parsimonious trees differed only in the branching order of NRRL 13818, 26156, and 28720 within *F. asiaticum*, and because the two strongly supported subclades collectively resolved seven of the nine *Fg* clade species. These include a South American subclade (100% bootstrap) comprising (*F. meridionale* (*F. austroamericanum* (*F. cortaderiae*, *F. brasilicum*))) and a second subclade (98% bootstrap) composed of (*F. acaciae-mearnsii*, *F. asiaticum* (*F. graminearum*)). However, the branching order and sister group relationship of these two subclades and the phylogenetic affinities of *F. boothii* and the Central American endemic *F. mesoamericanum* were unresolved (Fig. 6). Previously, *F. meridionale* and *F. acaciae-mearnsii* were considered to be endemic to Africa and *F. graminearum* to the Northern Hemisphere (O'Donnell et al., 2000). However, based on more extensive global sampling, *F. meridionale* appears to be endemic to South America, *F. acaciae-mearnsii* to Australia or less likely Africa while *F. graminearum* has a cosmopolitan distribution (data not shown). The latter species may also be a South American endemic based on the more even frequency of its three segregating trichothecene chemotypes in Brazil compared with those found in China and North America (Gale et al., unpublished). The endemic area of *F. boothii* is also problematical given its distribution in Africa, Mexico, and Mesoamerica.

Average *p*-distances calculated between *Fg* clade species (Kumar et al., 2001), using the combined dataset and sequence from the MAT locus in separate analyses, show that most species have diverged by about 1% (0.96–1.25% across all loci and 0.97–1.35% at MAT based on 30 of 36 comparisons, Table 4). However, the South American species *F. austroamericanum*, *F. meridionale*, *F. cortaderiae*, and *F. brasilicum* have diverged from one another by only 0.41–0.62% across all loci and by only 0.29–0.65% at the MAT locus. As expected, decay indices recorded for these four species, which ranged from 66 to 77, were the lowest for any species within the *Fg* clade. By comparison, *p*-distances between *F. culmorum* and *F. cerealis* are comparable to most of the *Fg* clade species, measuring 1.28 and 0.78% across all loci and the MAT locus, respectively. Estimates of DNA divergence between the *Fg* clade species (Table 4; Rozas et al., 2003) show that the greatest fraction of all polymorphism is fixed within a species. The strong negative correlation between shared polymorphism and fixed differences across the combined dataset (Table 4)

Table 4
Above diagonal: average *p*-distance between *Fg* clade species in the combined dataset and mating type data (in parentheses); below diagonal: fixed differences within and shared mutations between *Fg* clade species in the combined dataset and mating type data (in parentheses)

	F. austroamericanum	*F. meridionale*	*F. boothii*	*F. mesoamericanum*	*F. acaciae-mearnsii*	*F. asiaticum*	*F. graminearum*	*F. cortaderiae*	*F. brasilicum*
F. austroamericanum	—	0.0041 (0.0029)	0.0118 (0.0135)	0.0118 (0.0128)	0.0109 (0.0110)	0.0110 (0.0131)	0.0106 (0.0123)	0.0057 (0.0065)	0.0050 (0.0057)
F. meridionale	44/3 (22/3)	—	0.0122 (0.0131)	0.0121 (0.0128)	0.0111 (0.0108)	0.0112 (0.0124)	0.0109 (0.0119)	0.0062 (0.0063)	0.0042 (0.0036)
F. boothii	119/4 (58/2)	114/4 (59/2)	—	0.0099 (0.0127)	0.0096 (0.0119)	0.0108 (0.0105)	0.0102 (0.0097)	0.0113 (0.0135)	0.0114 (0.0128)
F. mesoamericanum	118/0 (64/0)	118/0 (68/0)	118/2 (53/1)	—	0.0100 (0.0121)	0.0125 (0.0131)	0.0114 (0.0109)	0.0111 (0.0126)	0.0117 (0.0126)
F. acaciae-mearnsii	127/0 (57/0)	105/2 (57/0)	131/1 (56/0)	134/1 (62/0)	—	0.0115 (0.0113)	0.0108 (0.0104)	0.0103 (0.0108)	0.0106 (0.0105)
F. asiaticum	130/1 (62/1)	101/2 (61/1)	130/3 (54/2)	138/0 (67/0)	112/0 (65/0)	—	0.0105 (0.0107)	0.0113 (0.0134)	0.0106 (0.0126)
F. graminearum	113/1 (59/1)	94/5 (61/1)	99/5 (38/2)	102/6 (45/2)	92/4 (56/0)	89/4 (58/2)	—	0.0106 (0.0120)	0.0102 (0.0115)
F. cortaderiae	32/1 (11/0)	54/1 (29/0)	124/0 (63/0)	121/0 (66/0)	129/0 (61/0)	134/1 (68/0)	118/0 (63/0)	—	0.0052 (0.0054)
F. brasilicum	42/0 (16/0)	59/0 (32/0)	132/0 (67/0)	131/0 (72/0)	138/0 (64/0)	142/0 (70/0)	124/0 (67/0)	41/0 (14/0)	—

indicates that recent gene flow between the species has been extremely limited. A similar pattern of genetic isolation emerges when these comparisons are extended to the single heterothallic and the four putatively asexual species (Table 5).

3.4. Phenotypic analysis and taxonomy

No differences were observed in colony characteristics of the different *Fg* clade species when compared on PDA in complete darkness at 25 °C. General features of the *Fg* clade colony and conidial phenotypes, including sparse or no chlamydospore production, matched published descriptions of *F. graminearum* (Booth, 1971; Gerlach and Nirenberg, 1982; Nelson et al., 1983; Wollenweber, 1931; Wollenweber and Reinking, 1935). Sizes (length and width) of 5-septate conidia were compared among the different *Fg* clade species and with representative strains of *F. cerealis*, *F. culmorum*, *F. lunulosporum*, and *F. pseudograminearum*. Based on average width of conidia, two groups of the *Fg* clade species were resolved (Fig. 7): Group A comprises

Table 5
Above diagonal: average *p*-distance between species in the combined dataset (12,161 bp) and the *MAT1-1* data (4442 bp, in parentheses); below diagonal: fixed differences within and shared mutations between species in the combined dataset and the *MAT1-1* data (in parentheses)

	F. cerealis	*F. culmorum*	*F. lunulosporum*	*F. pseudograminearum*	*Fusarium* sp. NRRL 29380
F. cerealis	—	0.0128 (0.0078)	0.0248 (0.0286)	0.0321 (0.0158)	0.0401 (0.0289)
F. culmorum	112/1 (19/0)	—	0.0246 (0.0262)	0.0324 (0.0139)	0.0391 (0.0271)
F. lunulosporum	248/0 (114/0)	260/0 (111/0)	—	0.0344 (0.0294)	0.0364 (0.0303)
F. pseudograminearum	334/1 (58/0)	352/0 (57/0)	358/0 (129/0)	—	0.0298 (0.0301)
Fusarium sp. NRRL 29380	445/0 (115/0)	446/0 (115/0)	395/0 (133/0)	328/0 (132/0)	—

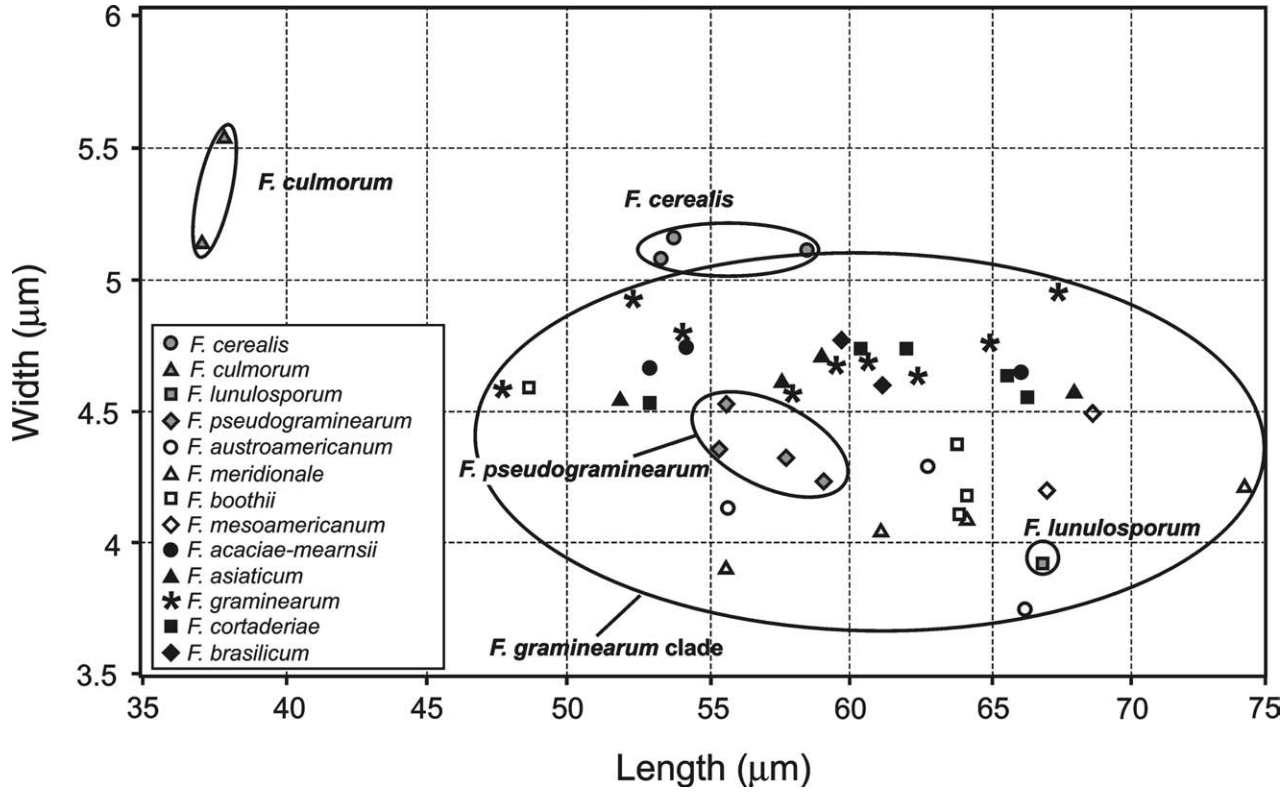

Fig. 7. Length and width of 5-septate conidia of *Fg* clade species cultured under continuous black light together with representative strains of *F. cerealis*, *F. culmorum*, *F. lunulosporum*, and *F. pseudograminearum*. Based on mean width of conidia, the *Fg* clade species formed two distinct groups: Group A represented by white symbols and Group B represented by black symbols. One strain of *F. boothii* NRRL 29011 is morphologically degenerate and represents an exceptional average value. Overlapping average values of conidial length and width for individual strains within either group show this character cannot be used exclusively for morphological species recognition.

F. austroamericanum, *F. meridionale*, *F. boothii*, and *F. mesoamericanum* represented by white symbols, while Group B comprises *F. acaciae-mearnsii*, *F. asiaticum*, *F. graminearum*, *F. cortaderiae*, and *F. brasilicum* represented by black symbols. Overlapping average values of conidial length, width, and widest positions for individual strains within each group demonstrate that these characters cannot be used individually for morphological species recognition (Table 6). However, when the most frequent conidial morphology of each species was considered (Table 6), three individual and three pairs of species could be distinguished within the *Fg* clade based on a combination of the following characters (Table 6, Fig. 7): conidial width, length of the longitudinal axis of conidia, presence or absence of a narrow apical conidial beak, morphological symmetry of the upper and lower halves of conidia, and the most frequent widest position of conidia.

Fusarium graminearum, which forms conidia mostly widest above the midregion, was unambiguously determined to be conspecific with *Fg* clade lineage 7 (O'Donnell et al., 2000) as the anamorph of *Gibberella zeae sensu str.* Conidial sizes of the Group B species precisely matched the size range for *F. graminearum* (5-septate: 51×4.9 μm on average) given by Wollenweber (1931) and Wollenweber and Reinking (1935), and conidial morphology of *F. asiaticum* and *F. graminearum* best matched the protologue of the species described therein. *Fusarium graminearum* is the only *Fg* clade species known from cereals in Europe and the United States, the respective type localities of *F. graminearum* and *G. zeae*. *Fusarium asiaticum*, by way of contrast, is only known from Asia and South America. This result adds to a growing list of fungal speciation studies that show genetic isolation precedes morphological differentiation (Chaverri et al., 2003; Taylor et al., 2000). In the descriptions that follow in Appendix A, each species is diagnosed primarily by fixed nucleotide characters listed by the gene, nucleotide position, and nucleotide.

4. Discussion

The primary objective of this study was to investigate the evolutionary history of the B trichothecene toxin-producing clade of *Fusarium*. Specifically, five

Table 6
Conidial morphology characteristic of each species within the B trichothecene toxin-producing clade of *Fusarium*[a]

Species	Width of 5-septate conidia (average value in μm)	Longitudinal axis of conidia	Narrow apical beak (+/-)	Upper and lower half of conidia	Widest region of conidia	Conidial morphology[b] 25 μm
F. austroamericanum	<4.5	Typically straight	+/-	Asymmetric	Midregion	
F. meridonale	<4.5	Gradually curved	+	Mostly symmetric	Midregion	
F. boothii	<4.5	Gradually curved	+	Mostly symmetric	Midregion	
F. mesoamericanum	4—4.5	Typically straight	-	Asymmetric	Above midregion	
F. acaciae-mearnsii	4.5—5	Gradually curved	+	Mostly symmetric	Below midregion	
F. asiaticum	4.5—5	Gradually curved	-	Asymmetric	Above midregion	
F. graminearum	4.5—5	Gradually curved	-	Asymmetric	Above midregion	
F. cortaderiae	4.5—5	Straight or gradually curved	+	Asymmetric	Below midregion	
F. brasilicum	4.5—5	Straight or gradually curved	+	Asymmetric	Below midregion	
F. lunulosporum	<4.5	Curved	+	Symmetric	Midregion	
F. pseudograminearum	4—4.5	Curved	+	Symmetric	Midregion	
F. cerealis	>5	Curved	+	Symmetric	Midregion	
F. culmorum	>5	Curved	-	Symmetric	Midregion	

[a] When the conidial characters were used collectively, the following three species and three species pairs could be distinguished within the *Fg* clade: *F. austroamericanum, F. mesoamericanum, F. acaciae-mearnsii, F. meridonale* + *F. boothii, F. asiaticum* + *F. graminearum*, and *F. cortaderiae* + *F. brasilicum*.

[b] All conidia were drawn from ex-holotype strains cultured on SNA under black light at 25 °C except for *F. graminearum* (NRRL 31084), *F. cerealis* (NRRL 13721) and *F. culmorum* (NRRL 3288).

interconnected questions were addressed: (1) Is heterothallism or homothallism the apomorphic condition within this clade?, (2) What is the nature of selective pressure impacting the evolution of the MAT genes?, (3) Are MAT gene trees also species trees?, (4) What is the phylogeny of the species?, and (5) Can genealogically concordant phylogenetic species within the *Fg* clade be diagnosed using phenotypic characters?

4.1. Evolution of MAT

In contrast to published results that support polyphyletic evolutionary origins of heterothallism in *Cochliobolus* (Yun et al., 1999), *Neurospora* and relatives (Dettman et al., 2001) and the *Fusarium solani* species complex (O'Donnell, 2000), results presented here support a monophyletic and apomorphic evolutionary origin of homothallism (self-fertility) within the B clade of *Fusarium.* Phylogenetic analyses of *mat A-1* and *mat* α-1 in *Neurospora* and *Sordaria* support a single evolutionary origin of homothallism within both genera (Pöggeler, 1999). However, heterothallism appears to be apomorphic within *Neurospora* while it may be pleisomorphic within *Sordaria*. The interpretation that heterothallism is the derived condition among *Aspergillus* species and associated *Neosartorya* teleomorphs did not take into account the possibility that species with unknown teleomorphs may be cryptically heterothallic or recently derived from heterothallic ancestors (Geiser et al., 1998a). All nine species within the *Fg* clade share a highly conserved MAT locus characterized by contiguous *MAT1-1* and *MAT1-2* idiomorphs (Fig. 1) with the full complement of MAT genes reported for pyrenomycetes (Turgeon and Yoder, 2000). Comparisons of B clade MAT loci with those of *F. verticillioides* and *F. proliferatum* (*Gibberella fujikuroi* species complex; O'Donnell et al., 1998a), and *F. oxysporum* (*F. oxysporum* species complex; O'Donnell et al., 1998b) show they are highly syntenic (Waalwijk et al., 2004) except that the *MAT1-1-2* gene in the B clade contains four introns (Yun et al., 2000) while only one intron is present within this gene in the latter two more closely related species. Surprisingly, genes that flank the MAT locus in *F. graminearum* are conserved in *Neurospora* and some ascomycetous yeasts (Butler et al., 2004). Homothallism within the *Fg* clade must have arisen in part from an unequal crossover event in their most recent common heterothallic ancestor, bringing the *MAT1-1* and *MAT1-2* idiomorphs together into the same locus, as previously proposed (Butler et al., 2004; Perkins, 1987). This interpretation is supported by the fact that their basal, heterothallic (self-sterile), and putatively asexual relatives possess *MAT1-1* and *MAT1-2* idiomorphs that are structurally identical to those within the *Fg* clade, albeit with only a single idiomorph per strain. Because this transition has been shown to require multiple steps in *Neurospora* (Glass and Smith, 1994), an unequal chromatid exchange bringing the two idiomorphs together within the same genome may be insufficient to transform a heterothallic species to one that is homothallic within this clade. However, strains of *F. graminearum* made heterothallic by the deletion of either idiomorph are able to outcross (Lee et al., 2003). The addition of 59 amino acids to the carboxyl-terminal portion of the *MAT1-1-2* protein, followed by a frameshift mutation within *F. boothii* that is predicted to result in 47 divergent amino acids at the carboxyl terminus, represents another apparent apomorphy in the evolution of the MAT locus in the *Fg* clade. These observations, together with the fact that interfertile strains of *Gibberella coronicola* lack these codons (Aoki and O'Donnell, 1999b), collectively indicate that the additional codons do not appear to be essential for sexual reproduction. Although the B clade *MAT1-1-3*, *MAT1-1-2*, and *MAT1-1-1* proteins show some similarity to *mat A-3*, *A-2*, and *A-1* of *N. crassa* and *Podospora anserina* (Kronstad and Staben, 1997; Turgeon and Yoder, 2000), respectively, targeted gene disruption experiments are needed to ascertain whether all three *MAT1-1* genes are essential for mating in *Fusarium*. Moreover, the possibility should also be considered that MAT genes might be involved in other functions such that the interpretation of experiments using MAT-null strains may not be straightforward.

Although a sexual state is unknown for four putatively asexual species within the B clade, three lines of evidence suggest that they may reproduce sexually: (1) idiomorphs of the four putatively asexual species are structurally identical to those found in the heterothallic *F. pseudograminearum* (*Gibberella coronicola*, Aoki and O'Donnell, 1999b) and translations of the MAT genes suggest that they encode functional proteins, (2) MAT genes appear to be under strong purifying selection, and (3) a preliminary survey of mating-types in *F. pseudograminearum*, and two putative asexuals, *F. culmorum* and *F. cerealis*, using *MAT1-1-1* and *MAT1-2-1* specific primers in a multiplex PCR, indicate that both idiomorphs occur in nearly equal frequencies on a global scale. The latter finding is consistent with frequency-dependent selection and sexual reproduction, as reported for other putative asexual pathogens (Linde et al., 2003, and references therein). However, hierarchal sampling at macro- and microgeographic scales is needed to accurately determine the distribution and frequency of mating types within these fusaria (Zhan et al., 2002). The *MAT1-1-1* and *MAT1-2-1* multiplex PCR assay should be useful in this regard, and because it worked on all members of the B clade, it should find utility in selecting partners of opposite mating type for in vitro sexual crosses.

The molecular evolutionary analyses presented here represent the first test of hypotheses regarding the

nature of selective pressure impacting the evolution of MAT genes. However, the results are consistent with those from the non-orthologous *b1* mating compatability gene found in *Coprinus cinereus* (May et al., 1999). The determination that observed levels of nonsynonymous substitutions are significantly less than neutral expectations demonstrate that MAT genes have been subject to strong purifying selection, and indicate that both the levels of polymorphism within species, and the evolutionary divergence of MAT genes following speciation, are constrained by the need to maintain the function of the MAT protein products. This finding is inconsistent with the conclusion of Turgeon (1998), based on a perceived lack of silent substitutions within the MAT genes of *Cochliobolus heterostrophus*, that MAT molecular evolution fits directly with patterns observed for other sex-related genes, including the mate-recognition genes of mollusks (Swanson and Vacquier, 1995) and echinoderms (Metz and Palumbi, 1996), which are characterized by high levels of nonsynonymous divergence and positive selection. However, Turgeon (1998) based this conclusion on the observation of only five nonsynonymous and two synonymous substitutions, and did not consider the relative rates of nonsynonymous and synonymous substitutions (d_N/d_S). Therefore, conclusions regarding the molecular evolution of MAT genes in *Cochliobolus* likely need to be reconsidered. The results presented here clearly demonstrate that MAT genes have been subject to strong purifying selection throughout the evolutionary history of the B clade fusaria. Similar comparative analyses for other ascomycetes are needed to determine if this is characteristic of MAT molecular evolution in general.

4.2. MAT and multilocus phylogeny of the B trichothecene clade

Phylogenetic analyses reported here, based on the combined DNA sequence data totaling 13.6 kb from eleven nuclear genes including the MAT locus, extend our knowledge of species limits and evolution within the B clade from previous studies (O'Donnell et al., 2000; Ward et al., 2002) through discoveries of: (1) two new phylogenetically distinct species, *Fusarium* sp. NRRL 29380 from Oregon (and NRRL 29298 from New Zealand, data not shown) *ex* orchard grass and *Fusarium brasilicum* from Brazil *ex* oats and barley; (2) a strongly supported South American subclade composed of (*F. meridionale* (*F. austroamericanum* (*F. cortaderiae*, *F. brasilicum*))), correcting our previous hypothesis that *F. meridionale* was an African endemic (O'Donnell et al., 2000), and a second subclade comprising (*F. acaciae-mearnsii*, *F. asiaticum* (*F. graminearum*)); (3) a monophyletic and apomorphic origin of homothallism within the B clade; and (4) highly concordant MAT and non-MAT phylogenies which strongly support the interpretation that the gene trees represent species trees. This latter finding supports the hypothesis that MAT genes may have utility in investigating species limits within the *Fg* clade (Yun et al., 2000). However, based on comparisons of PIC/bp and percent of variable positions for each partition, it is clear that the MAT genes are no more phylogenetically informative than most other genic regions, unless these comparisons are extended to the MAT intergenic regions. Surprisingly, the present GCPSR study is the first to our knowledge to compare the utility of all of the genic and intergenic regions within MAT for investigating species limits within any fungus. In addition to the present report, nucleotide sequences of the *MAT1-2-1* gene have been used to examine phylogenetic relationships within *Cochliobolus* (Berbee and Turgeon, unpublished in Turgeon, 1998), the *Gibberella fujikuroi* species complex (Steenkamp et al., 2000), and *Ascochyta* (Barve et al., 2003), primarily because degenerate primers have been designed to amplify the conserved HMG box from phylogenetically diverse fungi (Arie et al., 2000), and the *MAT1-1-1* gene has been used to infer the phylogeny of four species within the *Fg* clade found in Korea (Jeon et al., 2003). However, at least within the B trichothecene clade, *MAT1-2-1* and *MAT1-1-1* are the two least informative and most homoplasious MAT genic regions we sequenced. These results strongly suggest that it would be prudent to conduct a pilot experiment to ascertain what region(s) of MAT might provide the most phylogenetically informative variation before conducting a large-scale species level phylogenetic study.

Although outcrossing among the *Fg* clade species may occur in the laboratory (Bowden and Leslie, 1999), it is an insufficient predictor of species limits because sexual interfertility is a plesiomorphic character (Rosen, 1979). Moreover, results of the laboratory mating study (Bowden and Leslie, 1999) contrast with the lack of observed historical interbreeding clear in these results. For example, though a natural *F. meridionale* × *F. asiaticum* interspecific hybrid was found in Nepal (O'Donnell et al., 2000), the present phylogenetic results demonstrate that hybridization rates in the field have been insufficient to oppose differentiation by genetic drift as evidenced by the reciprocal monophyly of all nine *Fg* clade species. In addition, the high levels of segregation distortion observed in the genetic map constructed from a *F. asiaticum* (FRC R-5470 = NRRL 13819) and *F. graminearum* (GZ-3639 = NRRL 29169) cross (Jurgenson et al., 2002) is likely indicative of large-scale chromosomal rearrangements between the parental strains and is consistent with an interspecific cross (Rieseberg, 2001). This interpretation is also in agreement with genetic data from this cross and other independent sources: (1) karyotype analysis of *F. graminearum* and related species within the B clade

has clearly identified four chromosomes (Taga et al., 2003) rather than the nine linkage groups in the published linkage map (Jurgenson et al., 2002), (2) gene order established by linkage relationships for the published *F. asiaticum* × *F. graminearum* genetic map (Jurgenson et al., 2002) in many cases is in disagreement with that inferred from the whole genome sequence assembly of a *F. graminearum* (PH-1 = NRRL 31084) strain. By way of contrast, significant agreement exists between the physical and genetic maps based on a *F. graminearum* NRRL 31084 × *F. graminearum* NRRL 34097 cross (Gale et al., http://www.broad.mit.edu/annotation/fungi/fusarium/maps.html), and (3) in the *F. asiaticum* × *F. graminearum* cross, six of 54 polymorphic markers (>10%) were not found in the whole genome sequence of *F. graminearum*. This result means that a significant number of orthologs are not shared by parental strains of the *F. asiaticum* × *F. graminearum* cross. However, for the *F. graminearum* NRRL 31084 × *F. graminearum* NRRL 34097 genetic map, alleles for all 122 markers were found in both parents, and all but two of the markers were found in the whole genome assembly. One of the two 'missing' markers, the nuclear ribosomal intergenic region, was in the excluded reads of the *F. graminearum* sequencing project and the other, while found in both parents, was not represented in either the assembly or the excluded reads.

Leslie et al. (2001) suggested that the nine species lineages of the *Fg* clade represent subspecies. This idea was based on observations in the *Gibberella fujikuroi* species complex that isolates from different partially interfertile phylogenetic species tend to have AFLP band identity in the range of 40–65%, and *Fusarium asiaticum* and *F. graminearum* have approximately 50% AFLP identity. We advocate the formal recognition of species rather than subspecies for the nine lineages of the *Fg* clade, for the following reasons. First, we accept the potential for hybridization between species and do not require isolates of different species to be absolutely reproductively isolated, more in keeping with species concepts applied to plants and animals. Natural hybridization between closely related species is common in plants and animals and it serves as an important force behind adaptation and speciation (Burke and Arnold, 2001). Although it has been documented only in a handful of cases in the fungi (Brasier, 2001), this is likely the result of the widespread application of overly broad morphological species concepts. It is not surprising that morphologically indistinguishable sister species such as *F. asiaticum* and *F. graminearum* can form hybrids in the laboratory and produce fertile offspring (Bowden and Leslie, 1999), albeit with a reduction in fertility. As more species are diagnosed via GCPSR in fungi, we expect to see more evidence for natural hybridization uncovered, such as the discovery of hybrid individuals like *F. meridionale* × *F. asiaticum* strain NRRL 28721 (O'Donnell et al., 2000). Movement of cereal commodities around the world provides the opportunity for such hybridization events to occur, which may lead to the evolution of novel hybrid pathotypes (Brasier, 2001). One of the many benefits of GCPSR is that it allows recognition of hybridization events for what they are, which will in turn allow researchers to examine the effects of hybridization in the epidemiology and evolution of pathogenic and toxigenic fungi. Second, because of its objective population genetic and molecular evolutionary underpinnings, we propose that GCPSR provides a more reliable, easily portable, and biologically meaningful means for recognizing species boundaries than phenetic criteria such as percent identity of AFLP bands (Leslie et al., 2001). Third, it is unclear how subspecies should be defined and what they mean biologically. In summary, the lineages comprising the *Fg* clade show a clear history of reproductive isolation, and in addition show some level of intrinsic reproductive incompatibility as evidenced by their reduced fertility in artificial crosses, consistent with species concepts applied widely to plants and animals.

It is important to note that not all genes sampled within the B clade reflect the species phylogeny. Previously, we reported that evolution of genes encoding trichothecene biosynthesis within the B clade (Ward et al., 2002) has resulted in a novel example of a gene tree—species tree discordance due to: (1) nonphylogenetic sorting of ancestral polymorphism into extant species, and (2) maintenance of trans-specific polymorphism by balancing selection acting on trichothecene chemotype differences within the virulence-associated trichothecene mycotoxin gene cluster (Kimura et al., 2003). Even so, phylogenetic relationships and species limits within each of the three trichothecene chemotype clades are topologically concordant with the combined noncluster phylogeny as expected (Ward et al., 2002), given that allelic lineages of *het-c*, which are also under balancing selection (Wu et al., 1998), track with species limits. For this reason, it is inadvisable to use any of the genes within the trichothecene toxin gene cluster for phylogenetic inference within the B clade of *Fusarium*. However, in studies of species limits within *Stachybotrys* (Andersen et al., 2003; Cruse et al., 2002), a phylogeny inferred from the trichothecene gene *Tri5* was concordant with the other gene trees they constructed, and with toxin phenotype, too. Other evolutionary processes such as paralogy, incomplete lineage sorting, and interspecific hybridization, especially within multigene families such as the nuclear ribosomal DNA, have the potential to yield spurious species phylogenies (Ganley and Scott, 1998; Johannesson and Stenlid, 2003; O'Donnell and Cigelnik, 1997). One or more of these processes may have confounded accurate assessment of genetic relationships among *Fg* clade species from Nepal (Carter

et al., 2000) and Canada (Mishra et al., 2003), and within *F. culmorum* (Mishra et al., 2002) based on RFLP analysis of the nuclear ribosomal intergenic spacer (IGS) region. Phylogenetic reconstruction of an IGS dataset of the 47 strains analyzed in the present study, however, surprisingly revealed that the *Fg* clade, four of the *Fg* clade species and *F. culmorum* are all non-monophyletic within the IGS gene tree (O'Donnell, unpublished). This finding demonstrates that the IGS gene tree does not reflect evolution of the B trichothecene toxin-producing fusaria, and further illustrates the utility of GCPSR for detecting similar genealogical discordances (Taylor et al., 2000).

4.3. Phenotypic analysis and conclusions

Nine species were identified within the morphological species *F. graminearum* in the present study using GCPSR. The a posteriori phenotypic analysis revealed that only three of the nine *Fg* clade species could be diagnosed by a combination of conidial characters, suggesting that either strong stabilizing selection may be acting on the conidial phenotypes or insufficient evolutionary time has transpired for each species to have become differentiated morphologically. We have chosen to formally recognize them here, following the model of Fisher et al. (2002) and Couch and Kohn (2002) using fixed nucleotide differences, for the following reasons: (1) they fulfill the criteria of GCPSR because all nine *Fg* clade species were resolved as reciprocally monophyletic or exclusive groups in the combined phylogenetic analyses of eleven nuclear genes and three intergenic regions, (2) little or no phylogenetically informative polymorphism is shared among the species which is consistent with genetic isolation and an advanced state of biological speciation (Geiser et al., 1998b); (3) parsimony analysis of AFLP data is concordant with the DNA sequence data (Jeon et al., 2003); (4) in light of the cytological data clearly demonstrating that *F. graminearum* has four chromosomes (Taga et al., 2003), the genetic map with nine linkage groups based on a *F. asiaticum* × *F. graminearum* cross (Jurgenson et al., 2002) contrasts sharply with an intraspecific *F. graminearum* NRRL 31084 × *F. graminearum* NRRL 34097 cross (Gale et al., unpublished). Collectively, these data support the interpretation that the former is an interspecific cross, (5) even though additional species within the *Fg* clade are likely to be discovered in poorly sampled regions of the world, such as South America and Australia, they will not alter the taxonomic proposal presented here, and (6) given the importance of these pathogens to world agriculture, we feel that it is imperative to provide names for each species for the following two reasons: (i) to facilitate communication among plant pathologists, mycotoxicologists, and quarantine specialists so that active surveillance of their global movement and segregating trichothecene toxin chemotypes can be accurately reported, and (ii) to alert plant breeders of the importance of including representatives of each species in their breeding programs to increase the likelihood of developing new varieties with broad-based resistance to FHB. Our ongoing molecular epidemiological studies, using standardized marker loci, are directed at establishing a centralized database for the FHB species host and geographic distributions, and trichothecene chemotypes to facilitate these goals.

Acknowledgments

We thank Jody Robinson and Jean Juba for excellent technical assistance, Walter Gams for assistance with the Latin descriptions, Joe Bielawski for helpful discussions regarding maximum likelihood analyses, Steve Prather and Don Fraser for preparing the figures, Amy Morgan for synthesis of the primers, and the individuals and culture collections that generously supplied strains used in this study. K.O.D., T.J.W., and H.C.K. acknowledge the support of the US Wheat and Barley Scab Initiative. D.M.G. was supported by National Research Initiative Competitive Grant 2002-35201-12545. The mention of firm names or trade products does not imply that they are endorsed or recommended by the US Department of Agriculture over other firms or similar products not mentioned.

Appendix A

Species descriptions.

Fusarium austroamericanum T. Aoki, Kistler, Geiser et O'Donnell, sp. nov.

= *Fusarium graminearum*, lineage 1 sensu O'Donnell et al., Proc. Natl. Acad. Sci. USA 97 (2000) 7905–7910.

Anamorphus ut in *Fusario graminearum* in morphologia similis, sed distinguibilis characteribus sequentibus nucleotiditis fixationibus: mating type idiomorph positiones 411 (G), 591 (A), and 1634 (T); reductase positio 1144 (T); translation elongation factor (1α) positiones 207 (T), 427 (T), and 623 (A); ammonia ligase-1 positiones 350 (T), 862 (G), and 1120 (A); ammonia ligase-2 positio 539 (T); and β-tubulin-3 positio 192 (T).

Fusarium austroamericanum is morphologically similar to *F. graminearum*, but has slightly different conidial features from it and other species within the *Fg* clade. Sporodochial conidia formed by *F. austroamericanum* on SNA under black light are less than 4.5 μm wide on average and their dorsal and ventral lines are often parallel and straight. It is diagnosed by the following

uniquely fixed nucleotide characters: mating type idiomorph positions 411 (G), 591 (A), and 1634 (T); reductase position 1144 (T); translation elongation factor (1α) positions 207 (T), 427 (T), and 623 (A); ammonia ligase-1 positions 350 (T), 862 (G), and 1120 (A); ammonia ligase-2 position 539 (T); and β-tubulin-3 position 192 (T).

Distribution: South America (Brazil, Venezuela).

HOLOTYPUS: BPI 843473, a dried culture, collected in Brazil, date and host/substrate unknown, deposited in the herbarium of BPI, USA. Ex holotype culture: NRRL 2903, received from J. C. Lewis (WRRL, Albany, CA) in 1960 as *Polyporus circinatus* (Fr.) Fr. from Brazil and accessioned at NRRL. Other strains examined: NRRL 28585, NRRL 28718.

Etymology: austro- (Lat. Southern) + americanum (Lat. American); based on the geographic distribution of the species.

Fusarium meridionale T. Aoki, Kistler, Geiser et O'Donnell, sp. nov.

= *Fusarium graminearum*, lineage 2 sensu O'Donnell et al., Proc. Natl. Acad. Sci. USA 97 (2000) 7905–7910.

Anamorphus ut in *Fusario graminearum* in morphologia similis, sed distinguibilis characteribus sequentibus nucleotiditis fixationibus: mating type idiomorph positiones 471 (A), 498 (A), 609 (A), 945 (C), 981 (T), 1062 (G), 1559 (T), 2183 (G), 2294 (T), 2694 (G), 3285 (G), 4308 (T), and 4744 (G); reductase positiones 433 (C), 964 (T); translation elongation factor (1α) positiones 102 (C), 215 (T); *Tri101* positio 266 (T); phosphate permase-1 positio 383 (T); phosphate permase-2 positio 291 (T); ammonia ligase-1 positiones 577 (G), 677 (C), and 693 (G); and ammonia ligase-2 positiones 306 (T), 452 (A).

Fusarium meridionale is morphologically similar to *F. graminearum*, but has slightly different conidial features from it and other species within the *Fg* clade except *F. boothii*. Sporodochial conidia formed by *F. meridionale* on SNA under black light are less than 4.5 μm wide on average and their dorsal and ventral lines are often parallel and gradually curved, as in *F. boothii*. It is diagnosed by the following uniquely fixed nucleotide characters: mating type idiomorph positions 471 (A), 498 (A), 609 (A), 945 (C), 981 (T), 1062 (G), 1559 (T), 2183 (G), 2294 (T), 2694 (G), 3285 (G), 4308 (T), and 4744 (G); reductase positions 433 (C), 964 (T); translation elongation factor (1α) positions 102 (C), 215 (T); *Tri101* position 266 (T); phosphate permase-1 position 383 (T); phosphate permase-2 position 291 (T); ammonia ligase-1 positions 577 (G), 677 (C), and 693 (G); and ammonia ligase-2 positions 306 (T), 452 (A).

Distribution: South (Brazil) and Central America (Guatemala), South Africa, Australia, New Caledonia, Nepal, and Korea.

HOLOTYPUS: BPI 843474, a dried culture, from an orange twig, collected in New Caledonia, date unknown, deposited in the herbarium of BPI, USA. Ex holotype culture: NRRL 28436. Other strains examined: NRRL 28721, NRRL 28723, and NRRL 29010.

Etymology: *meridionale* (Lat. Southern); based on the current distribution of the species around the southern hemisphere.

Fusarium boothii O'Donnell, T. Aoki, Kistler et Geiser, sp. nov.

= *Fusarium graminearum*, lineage 3 sensu O'Donnell et al., Proc. Natl. Acad. Sci. USA 97 (2000) 7905–7910.

Anamorphus ut in *Fusario graminearum* in morphologia similis, sed distinguibilis characteribus sequentibus nucleotiditis fixationibus: mating type idiomorph positiones 760 (G), 893 (G), 918 (T), 1073 (C), 1878 (C), 2309 (T), 2498 (C), 2651 (C), 2874 (T), 3251 (T), 3379 (T), 3545 (A), 3564 (C), 3582 (A), 4808 (C), 5981 (T), and 6092 (C); reductase positiones 30 (G), 501 (T), 591 (G), 706 (C), 794 (C), and 919 (T); translation elongation factor (1α) positio 616 (C); histone H3 positiones 148 (C), 252 (C), 300 (T), and 404 (T); *Tri101* positiones 57 (G), 150 (G), 419 (T), 440 (T), 566 (A), 878 (C), 895 (T), 932 (T), 974 (T), 1032 (T), 1224 (A), 1292 (C), and 1305 (A); phosphate permase-1 positio 81 (A); ammonia ligase-1 positiones 197 (T), 560 (T), 662 (T), 674 (T), 693 (T), 863 (G), and 938 (G); β-tubulin-1 positio 445 (A).

Fusarium boothii is morphologically similar to *F. graminearum*, but has slightly different conidial features from it and other species within the *Fg* clade except *F. meridionale*. Sporodochial conidia formed by *F. boothii* on SNA under black light are less than 4.5 μm wide on average and their dorsal and ventral lines are often parallel and gradually curved, as in *F. meridionale*. It is diagnosed by the following uniquely fixed nucleotide characters: mating type idiomorph positions 760 (G), 893 (G), 918 (T), 1073 (C), 1878 (C), 2309 (T), 2498 (C), 2651 (C), 2874 (T), 3251 (T), 3379 (T), 3545 (A), 3564 (C), 3582 (A), 4808 (C), 5981 (T), and 6092 (C); reductase positions 30 (G), 501 (T), 591 (G), 706 (C), 794 (C), and 919 (T); translation elongation factor (1α) position 616 (C); histone H3 positions 148 (C), 252 (C), 300 (T), and 404 (T); *Tri101* positions 57 (G), 150 (G), 419 (T), 440 (T), 566 (A), 878 (C), 895 (T), 932 (T), 974 (T), 1032 (T), 1224 (A), 1292 (C), and 1305 (A); phosphate permase-1 position 81 (A); ammonia ligase-1 positions 197 (T), 560 (T), 662 (T), 674 (T), 693 (T), 863 (G), and 938 (G); and β-tubulin-1 position 445 (A).

Distribution: South Africa, Mexico, Guatemala, Nepal, and Korea.

HOLOTYPUS: BPI 843475, a dried culture, from *Zea mays* L. (corn), collected in South Africa, by P. Martin, date unknown, deposited in the herbarium of BPI, USA. Ex holotype culture: NRRL 26916 = CBS 316.73 = IMI 160243. Other strains examined: NRRL 29011, NRRL 29020, and NRRL 29105.

Etymology: *boothii*; after the fusariologist, Colin Booth.

Fusarium mesoamericanum T. Aoki, Kistler, Geiser et O'Donnell, sp. nov.

= *Fusarium graminearum*, lineage 4 sensu O'Donnell et al., Proc. Natl. Acad. Sci. USA 97 (2000) 7905–7910.

Anamorphus ut in *Fusario graminearum* in morphologia similis, sed distinguibilis characteribus sequentibus nucleotiditis fixationibus: mating type idiomorph positiones 335 (A), 357 (A), 704 (C), 793 (T), 807 (G), 815 (A), 817 (A), 886 (T), 1018 (A), 1343 (G), 1352 (T), 1366 (A), 1541 (A), 1737 (C), 1976 (A), 2167 (T), 2379 (C), 3168 (G), 3341 (A), 3634 (C), 3653 (T), and 6106 (T); reductase positiones 53 (G), 88 (G), 454 (A), 638 (A), 664 (T), 667 (T), and 857 (G); translation elongation factor (1α) positio 271 (A); histone H3 positiones 45 (T), 259 (G), and 261 (T); *Tri101* positiones 56 (T), 65 (T), 111 (G), 217 (T), 353 (A), and 1148 (A); phosphate permase-2 positio 35 (A); ammonia ligase-1 positiones 409 (G), 700 (T), 745 (C), and 1209 (T); ammonia ligase-2 positiones 94 (T), 286 (G), and 484 (C); β-tubulin-1 positiones 178 (T), 228 (C), and 367 (T); and β-tubulin-3 positiones 9 (T), 165 (T).

Fusarium mesoamericanum is morphologically similar to *F. graminearum*, but has slightly different conidial features from it and other species within the *Fg* clade. Sporodochial conidia formed by *F. mesoamericanum* on SNA under black light are 4–4.5 μm wide on average, often straight and frequently widest above the mid-region (Aoki and O'Donnell, 1999a). It is diagnosed by the following uniquely fixed nucleotide characters: mating type idiomorph positions 335 (A), 357 (A), 704 (C), 793 (T), 807 (G), 815 (A), 817 (A), 886 (T), 1018 (A), 1343 (G), 1352 (T), 1366 (A), 1541 (A), 1737 (C), 1976 (A), 2167 (T), 2379 (C), 3168 (G), 3341 (A), 3634 (C), 3653 (T), and 6106 (T); reductase positions 53 (G), 88 (G), 454 (A), 638 (A), 664 (T), 667 (T), and 857 (G); translation elongation factor (1α) position 271 (A); histone H3 positions 45 (T), 259 (G), and 261 (T); *Tri101* positions 56 (T), 65 (T), 111 (G), 217 (T), and 353 (A), 1148 (A); phosphate permase-2 position 35 (A); ammonia ligase-1 positions 409 (G), 700 (T), 745 (C), and 1209 (T); ammonia ligase-2 positions 94 (T), 286 (G), and 484 (C); β-tubulin-1 positions 178 (T), 228 (C), and 367 (T); and β-tubulin-3 positions 9 (T), 165 (T).

Distribution: Central America (Honduras) and Pennsylvania, USA ex *Cissus rhombifolia* (a Mesoamerican endemic).

HOLOTYPUS: BPI 843476, a dried culture, from a fruit of *Musa* sp., collected in Honduras, isolated by K. Alsøe, 4 Mar 1986, deposited in the herbarium of BPI, USA. Ex holotype culture: NRRL 25797 = CBS 415.86 = FRC R-8506 = IMI 309346. Other strains examined: NRRL 29148 = FRC R-4079.

Etymology: *meso-* (Lat. Central-) + *americanum* (Lat. American); based on the type locality of the species.

Fusarium acaciae-mearnsii O'Donnell, T. Aoki, Kistler et Geiser, sp. nov.

= *Fusarium graminearum*, lineage 5 sensu O'Donnell et al., Proc. Natl. Acad. Sci. USA 97 (2000) 7905–7910.

Anamorphus ut in *Fusario graminearum* in morphologia similis, sed distinguibilis characteribus sequentibus nucleotiditis fixationibus: mating type idiomorph positiones 85 (T), 515 (C), 764 (C), 781 (T), 980 (A), 1061 (C), 1071 (T), 1115 (A), 1166 (T), 1338 (A), 1484 (T), 2324 (A), 2328 (A), 2334 (A), 2557 (A), 2844 (T), 3258 (T), 3596 (C), 4726 (G), and 5023 (T); reductase positiones 68 (G), 445 (C), 465 (C), 754 (C), ad 1093 (A); translation elongation factor (1α) positiones 113 (C), 210 (C), and 416 (T); histone H3 positiones 282 (T), 371 (A); *Tri101* positiones 152 (G), 692 (T); phosphate permase-1 positio 358; phosphate permase-2 positiones 41 (C), 303 (G); ammonia ligase-1 positiones 105 (T), 107 (C), 108 (A), and 456 (T); ammonia ligase-2 positiones 194 (G), 467 (T); and β-tubulin-2 positiones 78 (T), 87 (T).

Fusarium acaciae-mearnsii is morphologically similar to *F. graminearum*, but has slightly different conidial features from it and other species within the *Fg* clade. Sporodochial conidia formed by *F. acaciae-mearnsii* on SNA under black light are 4.5–5 μm wide on average, gradually curved, and frequently widest below the mid-region. It is diagnosed by the following uniquely fixed nucleotide characters: mating type idiomorph positions 85 (T), 515 (C), 764 (C), 781 (T), 980 (A), 1061 (C), 1071 (T), 1115 (A), 1166 (T), 1338 (A), 1484 (T), 2324 (A), 2328 (A), 2334 (A), 2557 (A), 2844 (T), 3258 (T), 3596 (C), 4726 (G), and 5023 (T); reductase positions 68 (G), 445 (C), 465 (C), 754 (C), and 1093 (A); translation elongation factor (1α) positions 113 (C), 210 (C), and 416 (T); histone H3 positions 282 (T), 371 (A); *Tri101* positions 152 (G), 692 (T); phosphate permase-1 position 358; phosphate permase-2 positions 41 (C), 303 (G); ammonia ligase-1 positions 105 (T), 107 (C), 108 (A), 456 (T); ammonia ligase-2 positions 194 (G), 467 (T); and β-tubulin-2 positions 78 (T), 87 (T).

Distribution: Australia, South Africa.

HOLOTYPUS: BPI 843477, a dried culture, from *Acacia mearnsii* De Wild (black wattle), collected in Pietermaritzburg, South Africa, by Jolanda Roux, date unknown, deposited in the herbarium of BPI, USA. Ex holotype culture: NRRL 25754 = MRC 5120. Other strains examined: NRRL 26752, NRRL 26755, and NRRL 34207 = FRC R-4412 ex soil in Australia.

Etymology: *acaciae-mearnsii*; based on the host, *Acacia mearnsii*.

Fusarium asiaticum O'Donnell, T. Aoki, Kistler et Geiser, sp. nov.

= *Fusarium graminearum*, lineage 6 sensu O'Donnell et al., Proc. Natl. Acad. Sci. USA 97 (2000) 7905–7910.

Anamorphus in morphologia idem ac *Fusarium graminearum*, sed distinguibilis characteribus sequentibus nucleotiditis fixationibus: mating type idiomorph

positiones 267 (T), 530 (A), 770 (A), 946 (G), 860 (C), 961 (T), 1001 (T), 1137 (T), 1151 (T), 2533 (T), 2786 (T), 2839 (T), 3166 (G), 3763 (T), 3852 (G), 4224 (G), 4260 (T), 4838 (G), 5177 (T), 5297 (G), 5576 (C), 5932 (A), 6100 (A), and 6103 (A); reductase positiones 48 (A), 51 (A), 52 (A), 68 (C), 81 (C), 199 (A), 423 (G), and 582 (A); histone H3 positio 278 (G); *Tri101* positiones 212 (G), 389 (C), and 706 (A); phosphate permase-1 positio 35 (C); ammonia ligase-1 positiones 393 (T), 441 (T), and 573 (G); ammonia ligase-2 positio 177 (A); and β-tubulin-2 positio 399 (T).

Fusarium asiaticum is morphologically indistinguishable from *Fusarium graminearum*, but these two species have slightly different conidial features from other species within the *Fg* clade. Sporodochial conidia formed by *F. asiaticum* on SNA under black light are 4.5–5 μm wide on average, gradually curved and frequently widest above the mid-region (Aoki and O'Donnell, 1999a). It is diagnosed by the following uniquely fixed nucleotide characters: mating type idiomorph positions 267 (T), 530 (A), 770 (A), 946 (G), 860 (C), 961 (T), 1001 (T), 1137 (T), 1151 (T), 2533 (T), 2786 (T), 2839 (T), 3166 (G), 3763 (T), 3852 (G), 4224 (G), 4260 (T), 4838 (G), 5177 (T), 5297 (G), 5576 (C), 5932 (A), 6100 (A), and 6103 (A); reductase positions 48 (A), 51 (A), 52 (A), 68 (C), 81 (C), 199 (A), 423 (G), and 582 (A); histone H3 position 278 (G); *Tri101* positions 212 (G), 389 (C), and706 (A); phosphate permase-1 position 35 (C); ammonia ligase-1 positions 393 (T), 441 (T), and573 (G); ammonia ligase-2 position 177 (A); and β-tubulin-2 position 399 (T).

Distribution: Asia (China, Nepal, Japan, and Korea), South America (Brazil).

HOLOTYPUS: BPI 843478, a dried culture, isolated from a grain of *Hordeum vulgare* L. (barley), collected in Japan, date unknown, deposited in the herbarium of BPI, USA. Ex holotype culture: NRRL 13818 = FRC R-5469. Other strains examined: NRRL 6101, NRRL 26156, and NRRL 28720.

Etymology: *asiaticum* (Lat. Asian); based on the endemic area of the species.

Fusarium graminearum Schwabe—Flora Anhaltina 2285 (1838).

= *Fusarium graminearum*, lineage 7 sensu O'Donnell et al., Proc. Natl. Acad. Sci. USA 97 (2000) 7905–7910.

Teleomorphus: *Gibberella zeae* (Schweinitz) Petch, *Ann. Mycol.* 34 (1936) 260.

Mating type idiomorph positiones 305 (G), 1023 (A), 1111 (C), 1158 (T), 1206 (T), 1836 (A), 1998 (T), 2095 (G), 2397 (C), 2605 (C), 3381 (C), 5783 (T), and 5975 (G); reductase positio 113 (G), translation elongation factor (1α) positio 364 (C); histone H3 positio 279 (T); *Tri* 101 positiones 608 (T), 1176 (C); and β-tubulin-3 positio 156 (T).

Fusarium graminearum has slightly different conidial features from the other species within the *Fg* clade except *F. asiaticum*. Sporodochial conidia formed by *F. graminearum* on SNA under black light are 4.5–5 μm wide on average, gradually curved and frequently widest above the mid-region (Aoki and O'Donnell, 1999a). *Fusarium graminearum* is diagnosed by the following uniquely fixed nucleotide characters: mating type idiomorph positions 305 (G), 1023 (A), 1111 (C), 1158 (T), 1206 (T), 1836 (A), 1998 (T), 2095 (G), 2397 (C), 2605 (C), 3381 (C), 5783 (T), and 5975 (G); reductase position 113 (G), translation elongation factor (1α) position 364 (C); histone H3 position 279 (T); *Tri101* positions 608 (T), 1176 (C); and β-tubulin-3 position 156 (T).

Distribution: Cosmopolitan.

Strains examined: NRRL 5883, NRRL 6394, NRRL 13383, NRRL 28063, NRRL 28336, NRRL 28439, NRRL 29169, NRRL 31084, and NRRL 34097.

Fusarium cortaderiae O'Donnell, T. Aoki, Kistler et Geiser, sp. nov.

= *Fusarium graminearum*, lineage 8 sensu Ward et al., Proc. Natl. Acad. Sci. USA 99 (2002) 9278–9283.

Anamorphus ut in *Fusario graminearum* in morphologia similis, sed distinguibilis characteribus sequentibus nucleotiditis fixationibus: mating type idiomorph positiones 1871 (T), 2171 (G), 2619 (T), and 2802 (T); translation elongation factor (1α) positiones 91 (T), 96 (A), and 118 (A); *Tri101* positiones 316 (A), 464 (G), and 863 (T); ammonia ligase-1 positio 167 (A); ammonia ligase-2 positio 345 (A); β-tubulin-1 positio 529 (T); and β-tubulin-2 positio 30 (T).

Fusarium cortaderiae is morphologically similar to *F. graminearum*, but has slightly different conidial features from it and other species within the *Fg* clade except *F. brasilicum*. Sporodochial conidia formed by *F. cortaderiae* on SNA under black light are 4.5–5 μm wide on average, straight or gradually curved and frequently widest below the mid-region. It is diagnosed by the following uniquely fixed nucleotide characters: mating type idiomorph positions 1871 (T), 2171 (G), 2619 (T), and 2802 (T); translation elongation factor (1α) positions 91 (T), 96 (A), and 118 (A); *Tri101* positions 316 (A), 464 (G), and 863 (T); ammonia ligase-1 position 167 (A); ammonia ligase-2 position 345 (A); β-tubulin-1 position 529 (T); and β-tubulin-2 position 30 (T).

Distribution: South America (Argentina, Brazil), Oceania (Australia, New Zealand).

HOLOTYPUS: BPI 843479, a dried culture, from *Cortaderia selloana* Asch. et Graebn (pampas grass), collected in Henderson, AK, New Zealand, August 1965, by J. Dingley deposited in the herbarium of BPI, USA. Ex holotype culture: NRRL 29297 = ICMP 5435. Other strains examined: NRRL 29306, NRRL 31171, NRRL 31185, and NRRL 31205.

Etymology: *cortaderiae*; based on the host plant of the holotype.

Fusarium brasilicum T. Aoki, Kistler, Geiser et O'Donnell, sp. nov.

Anamorphus ut in *Fusario graminearum* in morphologia similis, sed distinguibilis characteribus sequentibus nucleotiditis fixationibus: mating type idiomorph positiones 471 (T), 3226 (T), 3505 (T), 4542 (A), 5480 (T), 5826 (T), and 6040 (A); reductase positiones 413 (G), 617 (G), 869 (A), and 937 (A); translation elongation factor (1α) positio 608 (G); phosphate permase-1 positio 78 (T); ammonia ligase-1 positiones 209 (C), 265 (T), and 823 (G); β-tubulin-1 positio 412 (G).

Fusarium brasilicum is morphologically similar to *F. graminearum*, but has slightly different conidial features from it and other species within the *Fg* clade except *F. cortaderiae*. Sporodochial conidia formed by *F. brasilicum* on SNA under the black light are 4.5–5 μm wide on average, straight or gradually curved and frequently widest below the mid-region. It is diagnosed by the following uniquely fixed nucleotide characters: mating type idiomorph positions 471 (T), 3226 (T), 3505 (T), 4542 (A), 5480 (T), 5826 (T), and 6040 (A); reductase positions 413 (G), 617 (G), 869 (A), and 937 (A); translation elongation factor (1α) position 608 (G); phosphate permase-1 position 78 (T); ammonia ligase-1 positions 209 (C), 265 (T), and 823 (G); and β-tubulin-1 position 412 (G).

Distribution: South America (Brazil).

HOLOTYPUS: BPI 843480, a dried culture, from *Avena sativa* L. (oats), collected in Brazil, 2000, by José Martinelli, deposited in the herbarium of BPI, USA. Ex holotype culture: NRRL 31281. Other strains examined: NRRL 31238.

Etymology: *brasilicum*; based on the type locality of the species.

References

Andersen, B., Nielsen, K.F., Thrane, U., Szaro, T., Taylor, J.W., Jarvis, B.B., 2003. Molecular and phenotypic descriptions of *Stachybotrys chlorohalonata* sp. nov. and two chemotypes of *Stachybotrys chartarum* found in water-damaged buildings. Mycologia 95, 1227–1238.

Aoki, T., O'Donnell, K., 1999a. Morphological characterization of *Fusarium pseudograminearum* sp. nov., formerly recognized as the Group 1 population of *Fusarium graminearum*. Mycologia 91, 597–609.

Aoki, T., O'Donnell, K., 1999b. Morphological characterization of *Gibberella coronicola* sp. nov., obtained through mating experiments of *Fusarium pseudograminearum*. Mycoscience 40, 443–453.

Arie, T., Kaneko, I., Yoshida, T., Noguchi, M., Nomura, Y., Yamaguchi, I., 2000. Mating- type genes from asexual phytopathogenic ascomycetes, *Fusarium oxysporum* and *Alternaria alternata*. Mol. Plant Microbe Interact. 13, 1330–1339.

Banke, S., Peschon, A., McDonald, B.A., 2004. Phylogenetic analysis of globally distributed *Mycosphaerella graminicola* populations based on three DNA sequence loci. Fungal Genet. Biol. 41, 226–238.

Barve, M.P., Arie, T., Salimath, S.S., Muehlbauer, F.J., Peever, T.L., 2003. Cloning and characterization of the mating type (*MAT*) locus from *Ascochyta rabiei* (teleomorph: *Didymella rabiei*) and a *MAT* phylogeny of legume-associated *Ascochyta* spp. Fungal Genet. Biol. 39, 151–167.

Booth, C., 1971. The Genus *Fusarium*. Commonwealth Mycological Institute, Kew, Surrey, England.

Bowden, R.L., Leslie, J.F., 1999. Sexual recombination in *Gibberella zeae*. Phytopathology 89, 182–188.

Brasier, C.M., 2001. Rapid evolution of introduced plant pathogens via interspecific hybridization. Bioscience 51, 123–133.

Burke, J.M., Arnold, M.L., 2001. Genetics and the fitness of hybrids. Annu. Rev. Genet. 35, 31–52.

Butler, G., Kenny, C., Fagan, A., Kurischko, C., Gaillardin, C., Wolfe, K.H., 2004. Evolution of the *MAT* locus and its Ho endonuclease in yeast species. Proc. Natl. Acad. Sci. USA 101, 1632–1637.

Carbone, I., Anderson, J.B., Kohn, L.M., 1999. Patterns of descent in clonal lineages and their multilocus fingerprints are resolved with combined gene genealogies. Evolution 53, 11–21.

Carter, J.P., Rezanoor, H.N., Desjardins, A.E., Nicholson, P., 2000. Variation in *Fusarium graminearum* isolates from Nepal associated with their host of origin. Plant Pathol. 49, 452–460.

Chaverri, P., Castlebury, L.A., Samuels, G.J., Geiser, D.M., 2003. Multilocus phylogenetic structure within the *Trichoderma harzianum/Hypocrea lixii* complex. Mol. Phylogenet. Evol. 27, 302–313.

Couch, B.C., Kohn, L.M., 2002. A multilocus gene genealogy concordant with host preference indicates segregation of a new species, *Magnaporthe oryzae*, from *M. grisea*. Mycologia 94, 683–693.

Craven, K.D., Hsiau, P.T.W., Leuchtmann, A., Hollin, W., Schardl, C.L., 2001. Multigene phylogeny of *Epichloë* species, fungal symbionts of grasses. Ann. Missouri Bot. Gard. 88, 14–34.

Cruse, M., Telerant, R., Gallagher, T., Lee, T., Taylor, J.W., 2002. Cryptic species in *Stachybotrys chartarum*. Mycologia 94, 814–822.

Dettman, J.R., Harbinski, F.M., Taylor, J.W., 2001. Ascospore morphology is a poor predictor of the phylogenetic relationships of *Neurospora* and *Gelasinospora*. Fungal Genet. Biol. 34, 49–61.

Dettman, J.R., Jacobson, D.J., Taylor, J.W., 2003a. A multilocus genealogical approach to phylogenetic species recognition in the model eukaryote *Neurospora*. Evolution 57, 2703–2720.

Dettman, J.R., Jacobson, D.J., Turner, E., Pringle, A., Taylor, J.W., 2003b. Reproductive isolation and phylogenetic divergence in *Neurospora*: comparing methods of species recognition in a model eukaryote. Evolution 57, 2721–2741.

Eriksson, T., 1998. AutoDecay ver. 4.0 (program distributed by the author). Department of Botany, Stockholm University, Stockholm.

Fisher, M.C., Koenig, G.L., White, T.J., Taylor, J.W., 2002. Molecular and phenotypic description of *Coccidioides posadasii* sp. nov., previously recognized as the non-California population of *Coccidioides immitis*. Mycologia 94, 73–84.

Ganley, A.R.D., Scott, B., 1998. Extraordinary ribosomal spacer length heterogeneity in a Neotyphodium endophyte hybrid: implications for concerted evolution. Genetics 150, 1625–1637.

Geiser, D.M., Dorner, J.W., Horn, B.W., Taylor, J.W., 2000. The phylogenetics of mycotoxin and sclerotium production in *Aspergillus flavus* and *Aspergillus oryzae*. Fungal Genet. Biol. 31, 169–179.

Geiser, D.M., Frisvad, J.C., Taylor, J.W., 1998a. Evolutionary relationships in *Aspergillus* section *Fumigati* inferred from partial hydrophobin and beta-tubulin DNA sequences. Mycologia 90, 831–845.

Geiser, D.M., Juba, J.H., Wang, B., Jeffers, S.N., 2001. *Fusarium hostae* sp. nov., a relative of *F. redolens* with a *Gibberella* teleomorph. Mycologia 93, 670–678.

Geiser, D.M., Pitt, J.I., Taylor, J.W., 1998b. Cryptic speciation and recombination in the aflatoxin-producing fungus *Aspergillus flavus*. Proc. Natl. Acad. Sci. USA 95, 388–393.

Gerlach, W., Nirenberg, H., 1982. The genus *Fusarium*—A pictorial atlas. Mitt. Biol. Bundesanst. Land- Forstwirtsch. Berlin-Dahlem 209, 1–406.

Glass, N.L., Smith, M.L., 1994. Structure and function of a mating-type gene from the homothallic species *Neurospora africana*. Mol. Gen. Genet. 244, 401–409.

Goldman, N., Yang, Z., 1994. A codon-based model of nucleotide substitution for protein-coding DNA sequences. Mol. Biol. Evol. 11, 725–736.

Jeon, J.-J., Kim, H., Kim, H.-S., Zeller, K.A., Lee, T., Yun, S.-H., Bowden, R.L., Leslie, J.F., Lee, Y.-W., 2003. Genetic diversity of *Fusarium graminearum* from maize in Korea. Fungal Genet. Newslett. 50 (Suppl.), 142 (Abstract).

Johannesson, H., Stenlid, J., 2003. Molecular markers reveal genetic isolation and phylogeography of the S and F intersterility groups of the wood-decay fungus *Heterobasidon annosum*. Mol. Phylogenet. Evol. 29, 94–101.

Jurgenson, J.E., Bowden, R.L., Zeller, K.A., Leslie, J.F., Alexander, N.J., Plattner, R.D., 2002. A genetic map of *Gibberella zeae* (*Fusarium graminearum*). Genetics 160, 1451–1460.

Kasuga, T., White, T.J., Koenig, G., McEwen, J., Restrepo, A., Castañeda, E., Lacaz, C. da S., Heins-Vaccari, E.M., de Freitas, R.S., Zancopé-Oliveira, R.M., Qin, Z., Negroni, R., Carter, D.A., Mikami, Y., Tamura, M., Taylor, M.L., Miller, G.F., Poonwan, N., Taylor, J.W., 2003. Phylogeography of the fungal pathogen *Histoplasma capsulatum*. Mol. Ecol. 12, 3383–3401.

Kimura, M., Tokai, T., O'Donnell, K., Ward, T.J., Fujimura, M., Hamamoto, H., Shibata, T., Yamaguchi, I., 2003. The trichothecene biosynthesis gene cluster of *Fusarium graminearum* F15 contains a limited number of essential pathway genes and expressed nonessential genes. Fed. Eur. Biochem. Soc. Lett. 539, 105–110.

Koufapanou, V., Burt, A., Taylor, J.W., 1997. Concordance of gene genealogies reveals reproductive isolation in the pathogenic fungus *Coccidioides immitis*. Proc. Natl. Acad. Sci. USA 94, 5478–5482.

Koufapanou, V., Burt, A., Szaro, T., Taylor, J.W., 2001. Gene genealogies, cryptic species, and molecular evolution in the human pathogen *Coccidioides immitis* and relatives (Ascomycota, Onygenales). Mol. Biol. Evol. 18, 1246–1258.

Kroken, S., Taylor, J.W., 2001. A gene genealogical approach to recognize phylogenetic species boundaries in the lichenized fungus *Letharia*. Mycologia 93, 38–53.

Kronstad, J.W., Staben, C., 1997. Mating type in filamentous fungi. Annu. Rev. Genet. 31, 245–276.

Kumar, S., Tamura, K., Jakobsen, I.B., Nei, M., 2001. MEGA2: molecular evolutionary genetics analysis software. Bioinformatics 17, 1244–1245.

Lee, J., Lee, T., Lee, Y.-W., Yun, S.-H., Turgeon, B.G., 2003. Shifting fungal reproductive mode by manipulation of mating type genes: obligatory heterothallism of *Gibberella zeae*. Mol. Microbiol. 50, 145–152.

Leslie, J.F., Zeller, K.A., Summerell, B.A., 2001. Icebergs and species in populations of *Fusarium*. Physiol. Mol. Plant Pathol. 59, 107–117.

Linde, C.C., Zala, M., Ceccarelli, S., McDonald, B.A., 2003. Further evidence for sexual reproduction in *Rhynchosporium secalis* based on distribution and frequency of mating-type alleles. Fungal Genet. Biol. 40, 115–125.

May, G., Shaw, F., Badrane, H., Vekemans, X., 1999. The signature of balancing selection: fungal mating compatability gene evolution. Proc. Natl. Acad. Sci. USA 96, 9172–9177.

McMullen, M.P., Jones, P.R., Gallenberg, D., 1997. Scab of wheat and barley: a re-emerging disease of devastating impact. Plant Dis. 81, 1340–1348.

Metz, E.C., Palumbi, S.R., 1996. Positive selection and sequence rearrangements generate extensive polymorphism in the gamete recognition protein bindin. Mol. Biol. Evol. 13, 397–406.

Miller, J.D., Greenhalgh, R., Wang, Y., Lu, M., 1991. Trichothecene chemotypes of three *Fusarium* species. Mycologia 83, 121–130.

Mishra, P.K., Fox, R.T.V., Culham, A., 2002. Restriction analysis of PCR amplified nrDNA regions revealed intraspecific variation within populations of *Fusarium culmorum*. FEMS Microbiol. Lett. 215, 291–296.

Mishra, P.K., Tewari, J.P., Clear, R.M., Turkington, T.K., 2003. Genetic differentiation and phylogeographic structure of *Fusarium graminearum* in Canada. Fungal Genet. Newslett. 50 (Suppl.), 147 (Abstract).

Myllys, L., Stenroos, S., Thell, A., Ahti, T., 2003. Phylogeny of bipolar *Cladonia arbuscula* and *Cladonia mitis* (Lecanorales, Euascomycetes). Mol. Phylogenet. Evol. 27, 58–69.

Nelson, P.E., Toussoun, T.A., Marasas, W.F.O., 1983. *Fusarium* Species: An Illustrated Manual for Identification. The Pennsylvania State University Press, University Park.

O'Donnell, K., 2000. Molecular phylogeny of the *Nectria haematococca—Fusarium solani* species complex. Mycologia 92, 919–938.

O'Donnell, K., Cigelnik, E., 1997. Two divergent intragenomic rDNA ITS2 types within a monophyletic lineage of the fungus *Fusarium* are nonorthologous. Mol. Phylogenet. Evol. 7, 103–116.

O'Donnell, K., Cigelnik, E., Nirenberg, I., 1998a. Molecular systematics and phylogeography of the *Gibberella fujikuroi* species complex. Mycologia 90, 465–493.

O'Donnell, K., Kistler, H.C., Cigelnik, E., Ploetz, R.C., 1998b. Multiple evolutionary origins of the fungus causing Panama disease of banana: concordant evidence from nuclear and mitochondrial gene genealogies. Proc. Natl. Acad. Sci. USA 95, 2044–2049.

O'Donnell, K., Kistler, H.C., Tacke, B.K., Casper, H.H., 2000. Gene genealogies reveal global phylogeographic structure and reproductive isolation among lineages of *Fusarium graminearum*, the fungus causing wheat scab. Proc. Natl. Acad. Sci. USA 97, 7905–7910.

Perkins, D.D., 1987. Mating type switching in filamentous ascomycetes. Genetics 115, 215–216.

Pöggeler, S., 1999. Phylogenetic relationships between mating-type sequences from homothallic and heterothallic ascomycetes. Curr. Genet. 36, 222–231.

Rehner, S.A., Buckley, E.P., 2003. Phylogenetic, biogeographic and population genetic approaches to the analysis of cryptic speciation in the entomopathogen. Fungal Genet. Newslett. 50 (Suppl.), 145 (Abstract).

Rieseberg, L.H., 2001. Chromosomal rearrangements and speciation. Trends Ecol. Evol. 16, 351–358.

Rosen, D.E., 1979. Fishes from the uplands and intermontane basins of Guatemala: revisionary studies and comparative geography. Bull. Am. Museum Nat. Hist. 162, 267–376.

Roux, J., Steenkamp, E.T., Marasas, W.F.O., Wingfield, M.J., Wingfield, B.D., 2001. Characterization of *Fusarium graminearum* from *Acacia* and *Eucalyptus* using β-tubulin and histone gene sequences. Mycologia 93, 704–711.

Rozas, J., Sánchez-DelBarrio, Messeguer, X., Rozas, R., 2003. DnaSP, DNA polymorphism analyses by the coalescent and other methods. Bioinformatics 19, 2496–2497.

Schardl, C.L., Craven, K.D., 2003. Interspecific hybridization in plant-associated fungi and oomycetes: a review. Mol. Ecol. 12, 2861–2873.

Steenkamp, E.T., Wingfield, B.D., Coutinho, T.A., Zeller, K.A., Wingfield, M.J., Marasas, W.F.O., Leslie, J.F., 2000. PCR-based identification of MAT-1 and MAT-2 in the *Gibberella fujikuroi* species complex. Appl. Environ. Microbiol. 66, 4378–4382.

Steenkamp, E.T., Wingfield, B.D., Desjardins, A.E., Marasas, W.F.O., Wingfield, M.J., 2002. Cryptic speciation in *Fusarium subglutinans*. Mycologia 94, 1032–1043.

Swanson, W.J., Vacquier, V.D., 1995. Extraordinary divergence and positive Darwinian selection in a fusagenic protein coating the acrosomal process of abalone spermatozoa. Proc. Natl. Acad. Sci. USA 92, 4957–4961.

Swofford, D.L., 2002. PAUP*. Phylogenetic analysis using parsimony (*and other methods). Version 4.0b10. Sinauer Associates, Sunderland, MA.

Taga, M., Waalwijk, C., Flier, W.G., Kema, G.H.J., 2003. Cytological karyotyping of somatic chromosomes from *Phytophthora infestans*, *Mycosphaerella graminicola*, and *Fusarium* spp. Fungal Genet. Newslett. 50 (Suppl.), 149 (Abstract).

Taylor, J.W., Jacobson, D.J., Kroken, S., Kasuga, T., Geiser, D.M., Hibbett, D.S., Fisher, M.C., 2000. Phylogenetic species recognition and species concepts in Fungi. Fungal Genet. Biol. 31, 21–31.

Turgeon, B.G., 1998. Application of mating type gene technology to problems in fungal biology. Annu. Rev. Phytopathol. 36, 115–137.

Turgeon, B.G., Yoder, O.C., 2000. Proposed nomenclature for mating type genes in filamentous ascomycetes. Fungal Genet. Biol. 31, 1–5.

Waalwijk, C., van der Lee, T., de Vries, I., Hesselink, T., Arts, J., Kema, G.H.J., 2004. Synteny in toxigenic *Fusarium* species: the fumonisin gene cluster and the mating type region as examples. Europ. J. Plant Pathol. (in press).

Ward, T.J., Bielawski, J.P., Kistler, H.C., Sullivan, E., O'Donnell, K., 2002. Ancestral polymorphism and adaptive evolution in the trichothecene mycotoxin gene cluster of phytopathogenic *Fusarium*. Proc. Natl. Acad. Sci. USA 99, 9278–9283.

Windels, C.E., 2000. Economic and social impacts of Fusarium head blight: changing farms and rural communities in the Northern Great Plains. Phytopathology 90, 17–21.

Wollenweber, H.W., 1931. Fusarium-Monographie. Fungi parasitici et saprophytici. Z. Parasitenkd. 3, 269–516.

Wollenweber, H.W., Reinking, O.A., 1935. Die Fusarien, ihre Beschreibung, Schadwirkung und Bekämpfung. Paul Parey, Berlin.

Wu, J., Saupe, S.J., Glass, N.L., 1998. Evidence for balancing selection operating at the *het-c* heterokaryon incompatibility locus in a group of filamentous fungi. Proc. Natl. Acad. Sci. USA 95, 12398–12403.

Xu, J., Vilgalys, R., Mitchell, T.G., 2000. Multiple gene genealogies reveal recent dispersion and hybridization in the human pathogenic fungus *Cryptococcus neoformans*. Mol. Ecol. 9, 1471–1481.

Yun, S.-H., Arie, T., Kaneko, I., Yoder, O.C., Turgeon, B.G., 2000. Molecular organization of mating type loci in heterothallic, homothallic, and asexual *Gibberella/Fusarium* species. Fungal Genet. Biol. 31, 7–20.

Yun, S.-H., Berbee, M.L., Yoder, O.C., Turgeon, B.G., 1999. Evolution of the fungal self-sterile reproductive life style from self-sterile ancestors. Proc. Natl. Acad. Sci. USA. 96, 5592–5597.

Yang, Z., 1997. PAML: a program package for phylogenetic analysis by maximum likelihood. CABIOS 13, 555–556.

Yang, Z., 1998. Likelihood ratio tests for detecting positive selection and application to primate lysozyme evolution. Mol. Biol. Evol. 15, 568–573.

Yang, Z., Nielsen, R., Goldman, N., Pedersen, A.-M.K., 2000. Codon-substitution models for heterogeneous selection pressure at amino acid sites. Genetics 155, 431–449.

Zhang, J., Rosenberg, H.F., Nei, M., 1998. Positive Darwinian selection after gene duplication in primate ribonuclease genes. Proc. Natl. Acad. Sci. USA 95, 3708–3713.

Zhan, J., Kema, G.H.J., Waalwijk, C., McDonald, B.A., 2002. Distribution of mating type alleles in the wheat pathogen *Mycosphaerella graminicola* over spatial scales from lesions to continents. Fungal Genet. Biol. 36, 128–136.